Fine structure in the excitonic emission of InAs/GaAs quantum dot molecules

G. Ortner,* I. Yugova,† G. Baldassarri Höger von Högersthal, A. Larionov,‡ H. Kurtze, D. R. Yakovlev, and M. Bayer
Experimentelle Physik II, Universität Dortmund, D-44221 Dortmund, Germany

S. Fafard,§ Z. Wasilewski, and P. Hawrylak
Institute for Microstructural Sciences, National Research Council, Ottawa, Canada K1A 0R6

Y. B. Lyanda-Geller and T. L. Reinecke
Naval Research Laboratory, Washington, D.C. 20375, USA

A. Babinski and M. Potemski
Grenoble High Magnetic Field Laboratory, MPI/FKF and CNRS, Boîte Postale 166, 38042, Grenoble Cedex 9, France

V. B. Timofeev‡ and A. Forchel
Technische Physik, Universität Würzburg, Am Hubland, D-97074 Würzburg, Germany
(Received 12 January 2004; revised manuscript received 5 October 2004; published 30 March 2005)

The exciton fine structure in self-assembled coupled quantum dots with barriers of varying widths is studied in detail. For narrow barriers we find doublet splittings of the molecule ground state exciton in magnetic field, while for wide barriers in some cases a multiplet of emission lines is observed. Pronounced anticrossings occur in the field dispersion of such a multiplet with details depending on the particular molecule geometry. Strong variations of the fine structure including avoided crossings are observed also for the excited states that arise from the coupling-induced splitting of the quantum dot *s*-shell excitons. Values for the exciton diamagnetic shifts and spin splittings as functions of barrier width are given.

DOI: 10.1103/PhysRevB.71.125335 PACS number(s): 71.35.Ji, 71.70.Ej, 71.70.Gm

I. INTRODUCTION

The concept of reduction of dimensionality of semiconductor structures has been extremely successful during the last two decades:[1] technological efforts have focused first on realization of quasi-two-dimensional quantum wells and have then shifted toward the fabrication of quasi-one- and quasi-zero-dimensional structures (quantum wires and quantum dots). This development has provided not only a variety of device applications with unprecedented performances, it has also resulted in the observation of a variety of basic phenomena from which detailed insight into quantum physics has been obtained. For these purposes model systems have been designed in which the properties of the confined carriers as well as their interactions have been tailored almost at will.

With the achievement of precisely controllable quantum structures, some interest has moved toward coupling of these systems, to create artificial matter and to obtain new functional units. For quantum dots, the simplest such unit is a molecule formed by two dot structures located close to each other. Coupled dot systems are interesting not only because of the potential to study quantum mechanical tunneling, they are also of high interest for the currently very active field of quantum information processing.[2] The realization of a quantum bit by either a charge or a spin in a quantum dot has attracted considerable attention, as this approach might lead the way toward a technique scalable up to large numbers of involved bits.[3] Through a quantum dot molecule a gate might be obtained by which controllable interactions between quantum bits may be established and basic logic operations may be performed.

Coupled dot structures can be fabricated by various techniques such as double cleaved edge overgrowth,[4] lateral patterning of double quantum wells,[5] or gating of two-dimensional electron gases.[6] Spectroscopic studies of these systems revealed coupling induced splittings on the order of 1 meV. For the fabrication of quantum dots the growth by self-assembly has been shown to provide structures of particularly high quality.[7] It was soon recognized that self-assembly is also well suited to fabricate vertically correlated quantum dot pairs:[8] when growing two layers in close vicinity so that they are separated from each other by a few-nanometer-wide barrier only, the strain surrounding a quantum dot in the first, lower layer enforces the location of another dot in the second, upper layer on top of the first dot. The relative positions of the two dot structures are therefore well defined. Up to now quite a few spectroscopic studies of the confined electronic states have been performed on such coupled quantum dot samples[8–10] and also on a single molecule level.[11] By fine tuning the growth technique (see below) it was possible to obtain ensembles of molecules, the photoluminescence spectra of which revealed a well-resolved shell structure under high optical excitation.[12]

Lateral patterning of as-grown samples has been very successful for studying single quantum dots,[13] and hence was applied also to isolate single molecule structures, to avoid the significant inhomogeneous broadening of array spectra. In these studies emission line doublets were observed in the energy range of the *s*-shell emission, with energy separations depending systematically on barrier width.[14] The spectroscopic data thus indicated quantum mechanically coherent coupling of the two quantum dots. To explain the data, a

simple model of an exciton in a quantum dot molecule was developed which captures the essential features of tunnel coupling while neglecting complications that might arise from details of the valence band structure,[15–18] for example.

We note that the data presented in Ref. 14 certainly did not provide a unique proof for molecule formation, in particular since they involved comparative studies of different samples. It might be argued that the two lines originate from two independent quantum dots, whose properties such as dot size and composition vary systematically with barrier width. Such a variation might arise from a systematic change of the strain surrounding the first dot, for example. Further, since the data had been obtained by interband spectroscopy, by which the "combined" behavior of electron and hole can be addressed only, no conclusive decision could be made whether the splitting arises from the tunneling of electron and of hole or whether, for example, the hole is localized in one of the dots due to its heavy mass, and only the electron shows a tunnel coupling.

Therefore we have worked on developing spectroscopic tools from which the coupling of the dots can be concluded by studies performed on a single molecule structure. It turned out that the fine structure of the exciton emission in an external magnetic field provided such a tool.[19] In these studies distinctive anticrossings have been observed in the exciton magnetic field dispersions, which can occur only if the dots are quantum mechanically coherently coupled. According to model calculations, these anticrossings occur for structures with a lateral displacement of the dots relative to each other. Further evidence for the coupling was obtained from measurements of the diamagnetic shift of the exciton emission with the magnetic field applied in the Voigt geometry. By such experiments the extension of the exciton wave function along the molecule axis is tested. As compared to single quantum dot data, the diamagnetic shift for the molecules is considerably larger, indicating a larger extension of the wave function due to carrier penetration through the barrier, providing a demonstration of coupling also for molecules of high symmetry.

In this paper, we detail the studies of the "bonding" exciton states in quantum dot molecules in order to develop a more systematic picture. In particular, we give further data for wide barrier samples and extend the investigations toward narrow barriers. We take a close look at the exciton fine structure splitting patterns for the different samples and derive the barrier width dependence of the diamagnetic shift and the Zeeman splitting. Also some data for the "antibonding" exciton states are presented.

The paper is organized as follows. In Sec. II we discuss the studied quantum dot molecule samples. We introduce the technique that allows us to address single molecule structures in Sec. III. The exciton states in the molecules are discussed in Sec. IV, based on detailed numerical calculations. In Sec. V we present and discuss the spectroscopic data obtained on the molecules in several subsections. The article is concluded in Sec. VI by an outlook on future studies by which the knowledge about the electronic states in these coupled dot systems could be advanced further.

II. QUANTUM DOT MOLECULE SAMPLES

The quantum dot molecules studied here have been fabricated by Stransky-Krastanov growth,[20] which was specifically adapted to obtain two quantum dots with geometries as similar as possible. When growing coupled quantum dots using the conventional growth scheme for single dot layers it had been noted that the vertical alignment of the dot structures is good but the two dots may have considerably different sizes aggravating a tunnel coupling.[12,21] To overcome this problem, the growth scheme was extended by a so-called In-flush procedure. After having grown a first layer of lens-shaped InAs quantum dots, this layer is covered by a 3-nm-wide GaAs protection layer. Afterward, the growth chamber is flushed with indium, due to which the upper part of the lens is razed off so that the dot shape becomes disklike. By doing so the homogeneity of the structure height within the ensemble is improved, which is essential since height variations are the most important origin of the inhomogeneous broadening of ensemble spectra. Then the GaAs barrier is deposited as well as the second InAs quantum dot layer plus another 3 nm GaAs protection layer. Thereafter the dot shape engineering by In flush is repeated. Finally, for optical studies the structures are capped by a 100-nm-wide GaAs layer.

One remark on the material composition: the molecule structures were grown such that the dots are nominally made from InAs, while the surrounding barriers are GaAs. By high-resolution microscopy studies of quantum dots it has been established, however, that an intermixing of Ga and In occurs, smoothing the sharpness of the confinement potential and reducing its depth.[22] For the In-flush technique this intermixing naturally will also occur. Correspondingly the barrier will not be pure GaAs, but will have also a considerable In content. Since we do not have precise information on the composition, we will still refer to them as InAs/GaAs structures, although one has to be aware of the intermixing, in particular if one aims at a quantitative modeling of the observed phenomena.

Samples with nominal barrier widths d of 4, 5, 6, 7, and 8 nm have been prepared. Here, barrier width means the distance from the top of the lower wetting layer to the bottom of the upper wetting layer. To allow for comparison, also a sample with a 16-nm-wide barrier and a sample containing only a single dot layer have been grown. Figure 1 shows a transmission electron micrograph of a molecule structure with a barrier of 6 nm nominal width.[23] The size homogeneity of the dots is good: they are disk shaped with a height of $\sim 2 \pm 1$ nm and a diameter of $\sim 20 \pm 5$ nm. From the quantum dot heights we estimate the effective width of the barrier between the two dots to be 1–2 nm smaller than the nominal width.

Microscopy studies also suggest that up to the largest barrier widths studied here the vertical correlation of the two quantum dots is quite distinctive: Whenever a quantum dot appears in the first layer, there is also a quantum dot in the second layer. Further, precise information about the positions of the dot structures relative to each other has been established: for narrow barriers such as 4 and 5 nm the vertical alignment of the dots in all cases is good, while for wider barriers (7 and 8 nm) with considerable probability lateral

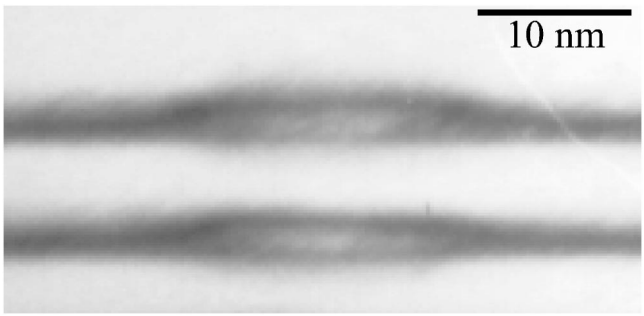

FIG. 1. Transmission electron micrograph of a single InAs/GaAs quantum dot molecule with a nominal barrier width of 6 nm (from wetting layer to wetting layer). The 10 nm bar gives the vertical and horizontal length scales.

displacements of the dots up to a few nanometers are observed, as reported earlier.[14,19]

Figure 2 shows photoluminescence spectra of arrays of quantum dot molecules with barrier widths of 4, 5, and 6 nm as compared to the single dot layer sample. Varying excitation powers were used to record these traces. For the single dot layer, only emission from the *s* shell is observed at low excitation powers. With increasing excitation the ground states are completely filled and carriers have to occupy the excited states due to Pauli blocking. Consequently, emission from the *p* shell appears in the spectra. Also for the quantum dot molecules, in all cases a shell structure is resolved as the inhomogeneous broadening is small enough. Let us first compare the results for the 5 nm barrier sample with the ones obtained for the dot reference. For the molecules, we observe

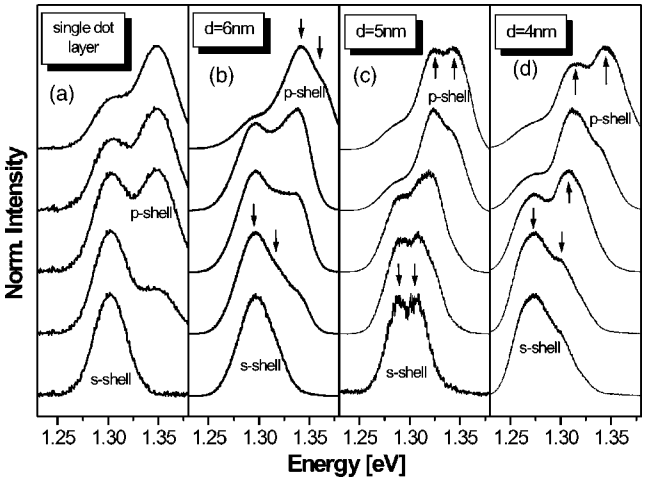

FIG. 2. Photoluminescence spectra of arrays of InAs/GaAs quantum dot molecules with nominal barrier widths of 4, 5, and 6 nm (the three righthand panels) as compared to corresponding spectra of a single dot layer reference sample (the left panel). Various excitation power levels were used to record these emission traces at $T=2$ K: From bottom to top the excitation power P_{exc} was increased from 0.1 to 0.2, 0.5, 1, and finally 2 mW. In conjunction with a laser spot diameter of about 20 μm these powers correspond to excitation densities of 32, 64, 160, 320, and 640 W cm^{-2}, respectively. The arrows indicate the tunnel split quantum dot shells in the molecules.

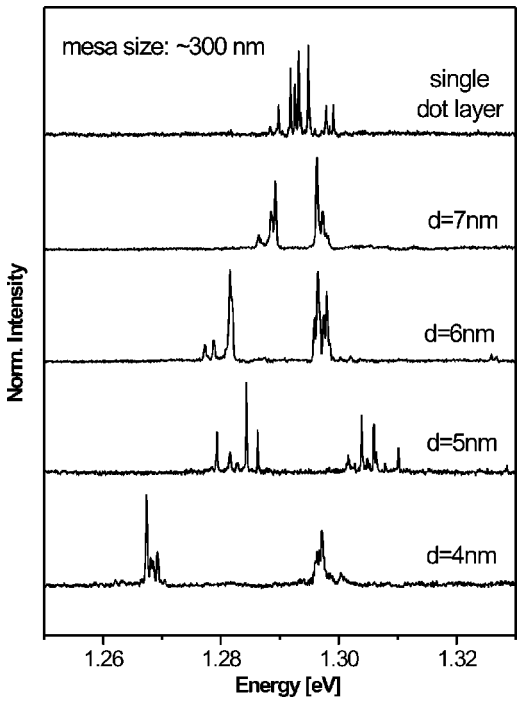

FIG. 3. Photoluminescence spectra of InAs/GaAs quantum dot molecules of varying barrier widths *d* recorded on mesa structures with a lateral size of ~300 nm, in comparison to a corresponding spectrum from the single dot layer sample ($T=10$ K). The excitation power density was $P_{\mathrm{exc}}=50$ W cm^{-2} for all traces.

at rather low excitation (see below) a splitting of the *s*-shell emission into two features, separated by ~25 meV. Upon increasing excitation, emission from the *p* shell appears, for which also a splitting is observed which is slightly larger than that of the *s* shell (~30 meV).

Also for the coupled dot samples with barrier widths of 4 and 6 nm we observe indications for a splitting of the *s*-shell and *p*-shell emissions as indicated by the arrows in the spectra of Fig. 2. However, the splittings cannot be resolved so clearly since for the 6 nm barrier sample the *s*-shell splitting, for example, appears to be small as compared to the inhomogeneous broadening so that the split emission lines strongly overlap. This is even more the case for the samples with 7 and 8 nm barriers, where no signatures for a splitting are seen in the array emission, except for a broadening of the emission bands as compared to the single layer emission. On the other hand, for the 4 nm barrier sample the splitting of the molecular levels appears to be so much enlarged that the high-energy *s*-shell emission line has significant overlap with the low-energy emission line of the *p* shell.

III. EXPERIMENTAL TECHNIQUE

To study single quantum dot molecules on these high-structural-density samples (estimated density ~10^{10}cm^{-2}), the as-grown probes were patterned laterally to form square-shaped mesa structures with varying lateral sizes down to below 100 nm. Details of the patterning technique have been given earlier.[24] Figure 3 shows spectra of samples with dif-

ferent barrier widths that were recorded at $T \sim 10$ K on mesa structures with lateral sizes of ~300 nm. The excitation power was adjusted to a level that the *s*-shell states are occupied, while the *p*-shell occupation is negligible. From these traces the indications for a tunneling-induced splitting of the quantum dot shells are consolidated. Clearly, the *s*-shell emission splits into two sets of sharp emission lines for the molecules, among which the energy separation strongly increases with decreasing barrier width.

The splitting pattern thus very much follows the intuitive picture of the formation of bonding and antibonding molecule orbitals due to tunnel coupling. The symmetry character of the exciton states will be discussed in more detail below. When reducing the excitation power, the intensity from the higher-lying features becomes slightly weaker, but emission from both *s*-shell states is observed even for very low excitation powers. That observation indicates a reduced energy relaxation rate of carriers between the tunnel-split states, even though the relaxation from *p*-shell to *s*-shell states appears to be fast.[25] This goes in line with the observation of rather narrow emission linewidths for the higher-lying states (<1 meV).[26]

The origin of this relaxation reduction between the tunneling-split exciton states is not clear yet. At very low excitation powers carrier-carrier scattering cannot contribute, so that relaxation can occur through phonon emission only. Except for the 4 nm barrier sample for which the shell splitting becomes comparable to the energy of the optical phonons (see Fig. 5 below), for all the other studied structures the splitting between these states is smaller than the optical phonon energy. Therefore only emission of acoustic phonons is possible. For it, the carrier relaxation rate is expected to be considerably smaller than for LO-phonon emission. If the relaxation time becomes comparable to or even longer than the radiative decay time of the excitons, emission will appear also from the "antibonding" states.

Figure 4 gives photoluminescence spectra at $T = 10$ K for mesa structures of different sizes as compared to the spectrum of an effectively unpatterned 5-μm-wide reference, all with a 5 nm barrier. When reducing the mesa size the number of spectral lines in the two split *s*-shell emission bands is reduced as evidenced is going from the 600- to the 150-nm-wide mesa. For the smallest mesa with a nominal size of 80 nm we find two dominant emission lines only, which are split by about 25 meV. When adjusting the laser spot on this mesa, the intensities of the two lines show strong correlations. We take the entirety of these observations as indication for a mesa occupancy by a single molecule structure. Also an emission spectrum of the same mesa structure recorded at ~50 K is shown (bottom trace in Fig. 4).[27] In order to still have strong emission intensity from the "bonding" state, the excitation power had to be increased, leading to a slight increase of the intensity from the antibonding state.[28] Similar spectra were chosen for presentation in Ref. 14.

We note that mesa structures with sizes smaller than ~100 nm are found, for which the emission spectra consist of more than two intense lines, for example three or four lines. Based on the spectroscopic tools applied here, it cannot be decided whether these emission patterns originate from a single molecule only (see below). On the other hand, we also

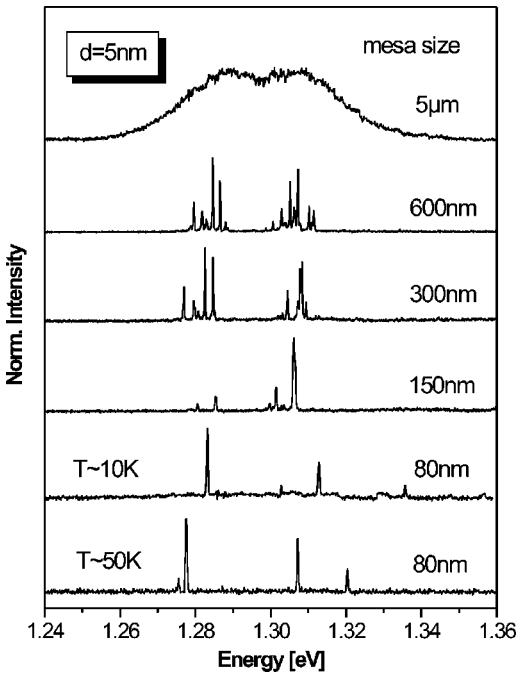

FIG. 4. Photoluminescence spectra recorded at rather low optical excitation power for 5 nm barrier InAs/GaAs quantum dot molecules ($P_{exc} \approx 40$ W cm^{-2}, except for the bottom trace where $P_{exc} \approx 200$ W cm^{-2}). The top trace gives the emission of a 5-μm-large field which is basically identical to that of the unpatterned reference sample; the other traces give the emissions from mesas of different lateral sizes as indicated at each spectrum. All traces were measured at 10 K, except for the lowest one recorded at ~50 K.

note that in some cases emission from a single quantum dot (QD) molecule is believed to be detected when a doublet of closely spaced emission lines with a splitting in the meV range appears in the spectra for the "bonding" exciton state (see the discussion of QDM5 below).

From spectra such as the ones presented in Figs. 2–4 the barrier width dependence of the emission line splittings for the *s* and the *p* shell in Fig. 5 can be derived. The bars indicate the variation of the splitting for a given *d*, as derived from a large number of studied mesa structures. For better resolution of this variation, the *p*-shell splittings have been shifted by 0.2 nm to lower barrier widths, so that the corresponding bars do not overlap with those for the *s*-shell splittings. For a particular sample the absolute energies of the emission features vary when moving the laser across the wafer. This is exemplified in Fig. 6 for the 4 nm barrier sample which shows emission spectra recorded on 300-nm-wide mesa structures that were located at different positions of the wafer. Despite the "global" variations on the wafer, locally the splitting between the lines is rather insensitive. This shows that there are no strong variations of the QD geometries for different molecules within a particular mesa.

The average splitting increases systematically with decreasing barrier width,[29] even though it shows quite some fluctuations (see Fig. 5), since the underlying single particle tunnel matrix elements, for example, depend exponentially on barrier width and height. Therefore only tiny variations of the barrier are translated into considerable changes of the

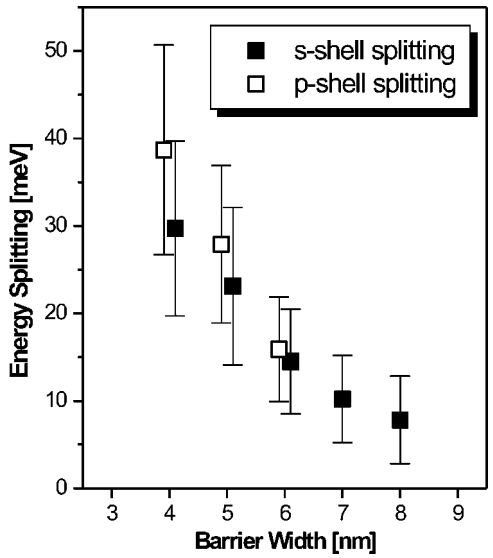

FIG. 5. Energy splittings of the *s*- and *p*-shell emission features of the quantum dot molecules versus nominal barrier width (the full and open symbols, respectively). The bars indicate the variation of splittings observed on different mesa structures. The *p*-shell splittings have been shifted by 0.2 nm to smaller barrier widths, so that the bars for *s* and *p* shells do not overlap, for better visualization. The data for the *p* shell have been derived from ensemble measurements on unpatterned samples or on large mesas. For them high-excitation spectra have been analyzed by multi-Gaussian line-shape fits to determine the splittings.

tunnel splitting. The sensitivity to these parameters becomes larger, the narrower the barrier is, causing a strong increase of the tunnel-splitting fluctuations.

For the exciton splitting, the tunnel matrix elements become renormalized by electron-hole Coulomb interactions. For the studied samples the tunnel coupling and the Coulomb coupling are of comparable magnitude. As they are not negligible, both need to be included for an adequate theoretical description. Therefore neither a single particle picture nor a picture of exciton tunneling seems appropriate to describe the coupling in the molecules. Both these models are limiting cases, which in the experiment might be approached for very narrow and very wide barriers, respectively.

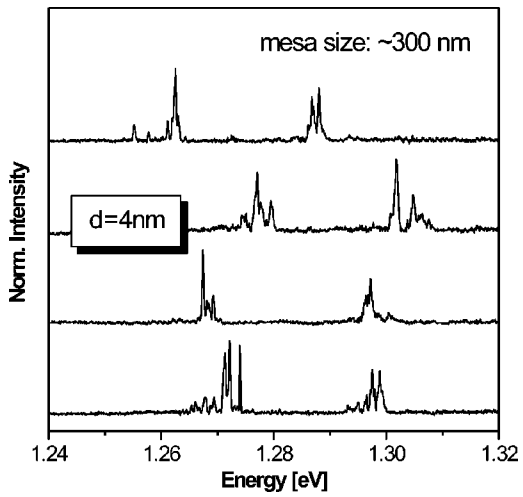

FIG. 6. Photoluminescence spectra of different mesa structures, all with a nominal lateral size of 300 nm, located at different positions of the quantum dot molecule sample with a 4 nm barrier ($T=10$ K). The excitation power density was 40 W cm^{-2}.

Independent of any modeling, the dot shell splittings are rather large as compared to other coupled dot systems and may even exceed the thermal energy at room temperature for the narrow barrier samples. Further, the *p*-shell splittings are systematically larger than the splittings observed for the *s* shell: energetically higher-lying states have a stronger penetration through the barrier resulting in a larger tunneling matrix element and thus a larger splitting of the energy levels. When compared to theoretical calculations the observed splittings are, however, somewhat smaller than the calculated ones.[18,30] This discrepancy might indicate problems in the right choice of material parameters. For example, for the carrier masses too small values corresponding to pure InAs might be used, in particular for the electron. Intermixing will cause an effective InGaAs composition leading to a considerable increase of this mass, and to a strong reduction of the tunnel matrix element. Also the width of the barriers might be estimated as too small.

For the fine structure studies, the samples were immersed at $T=2$ K in the liquid helium insert of an optical magnetocryostat ($B \leqslant 8$ T). The orientation of the sample relative to the field direction defined by the split coil of the magnet was variable, so that B could be applied along or normal to the heterostructure growth direction (in the following termed the Faraday and Voigt configurations, respectively). A frequency-doubled $NdYVO_4$ laser was used for optical excitation. The sample was imaged into an intermediate plane (for control of focusing on a mesa structure and, even more important, to suppress stray light by a small aperture). The emission was then focused onto the entrance slit of a single or double grating monochromator ($f=0.5$ m) and detected by a liquid nitrogen cooled charge-coupled device camera. The polarization of the emission could be analyzed by a proper combination of linear polarizers and quarter-wave plates.

Before we turn to the discussion of the data for the molecule samples, we present briefly the data for the single quantum dot layer sample as well as for the sample with a 16 nm barrier. The fine structure splitting pattern observed on single dots is qualitatively identical to the patterns that have been comprehensively discussed in Ref. 31 and in studies from other authors (see references in Ref. 31): The zero-field exciton emission lines show mostly a doublet splitting in magnetic field which depends linearly on B. In a few cases a quadruplet splitting is observed, which is attributed to an activation of the dark exciton states with angular momentum $|M|=2$ along the heterostructure growth direction, where M is the sum of electron and hole momenta (see also the discussion below). This activation occurs through mixing with the bright excitons with $|M|=1$ which might be caused by structural asymmetries or might be magnetic field induced.[31,32]

Turning to the 16 nm barrier sample: for this wide barrier the tunneling matrix elements are expected to be negligibly small, so that the dot structures have to be treated as decoupled, even though there is still a strong vertical correlation of

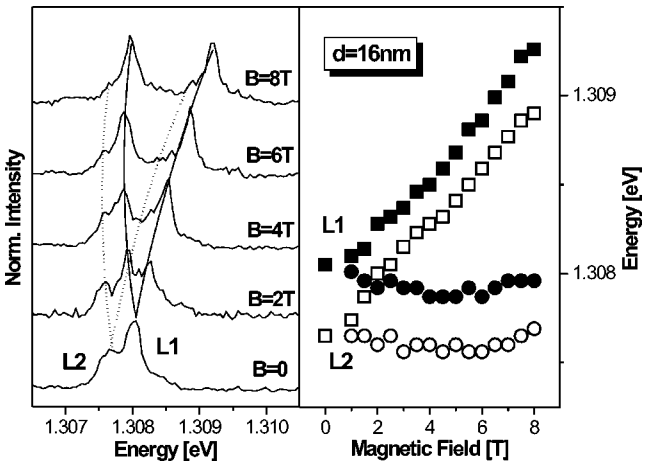

FIG. 7. Left panel: Photoluminescence spectra recorded at $T=2$ K on a pair of InAs/GaAs quantum dots separated by a barrier of 16 nm nominal width for different magnetic fields (Faraday configuration). The solid and dotted lines are guides to the eye. Right panel: The resulting exciton transition energies versus magnetic field.

quantum dot positions as seen from electron microscopy. An example of photoluminescence spectra recorded on a mesa structure prepared on this sample is shown in Fig. 7, left panel. At $B=0$ two emission lines L_1 and L_2 are observed, which have strongly different emission intensities. This indicates that the carrier capture efficiency into the two quantum dots is different. The splitting between the two lines is ~ 0.4 meV only. From the magnetic field dependence of the fine structure splitting it can be excluded that the low-energy line corresponds to a predominantly dark exciton state: each of the two emission lines splits into a doublet when applying B, and the intensities of the low-energy doublet features become even weaker so that they are hardly resolvable at high B. The splittings of the two doublets are identical for all field strengths (right panel of Fig. 7), preventing the dark exciton interpretation, since bright and dark excitons would have different g factors, as long as neither the electron nor the hole g factor is zero. Further, when the low-energy line emerging from L_1 and the high-energy line emerging from L_2 come into resonance, they seem to cross each other within the experimental accuracy, excluding any coupling between the dots.

IV. EXCITON STATES IN COUPLED QUANTUM DOTS

In Ref. 14 we have developed a simple model for the exciton states in molecules, which arise from the ground state exciton of an isolated quantum dot through tunnel coupling. For that purpose, we have indexed the lower and upper dots by 0 and 1, respectively. In an independent particle picture, the electron and hole can be distributed in four different ways among the two dots: they can be located in the same dot resulting in the configurations $|0,0\rangle$ and $|1,1\rangle$, where the first (second) index in the state vector gives the position of the electron (hole). Further, electron and hole can be located in opposite dots corresponding to the configurations $|0,1\rangle$ and $|1,0\rangle$. Including the Coulomb interaction between electron and hole leads to a mixing of these four configurations, so that the general form of the four exciton wave functions is given by

$$|S_i\rangle = c_{i,1}|0,0\rangle + c_{i,2}|1,1\rangle + c_{i,3}|0,1\rangle + c_{i,4}|1,0\rangle,$$

$$i = 1,\ldots,4. \tag{1}$$

The weight of each single particle configuration in this form is determined by the molecule parameters. Let us first discuss the case of an ideal molecule structure consisting of identical dots that are perfectly aligned relative to each other. The molecule structure therefore has inversion symmetry with respect to its center plane (taken as $z=0$).[33] This symmetry is reflected also by the exciton wave functions. For calculating them in an effective mass model, the following set of material parameters was chosen. The height of the dots was taken to be 1.2 nm. For the electron (hole) confinement potentials we assumed 680 meV (100 meV). For the carrier masses we used $0.04m_0$ for electrons in the dot and $0.067m_0$ outside. For the holes the same masses were used inside and outside the dot structures, $0.34m_0$ along the molecule axis, and $0.04m_0$ perpendicular to this axis. From these parameters in-plane quantization energies of 23 and 22 meV are obtained for electron and hole, respectively.

The four exciton states arising from the s-shell exciton splitting of an isolated quantum dot are shown in Fig. 8 for a molecule with a 5-nm-wide barrier: The lower panels give the two low-energy states $|S_1\rangle$ (left hand) and $|S_2\rangle$ (right hand), the upper panels give the high-energy states $|S_3\rangle$ (left hand) and $|S_4\rangle$ (right hand). In each case the vertical axis gives the amplitude of the wave function, while the in-plane axes give the coordinates of electron and hole along the molecule axis z. The electron and hole coordinates in the quantum dot molecule plane are held constant and in particular are set equal to zero. The peaks in the panels correspond to the different single particle configurations.

The weights of these configurations are determined by the interplay of Coulomb interaction and tunnel coupling matrix elements, v and t, respectively. For the particular structure under study with a narrow barrier $t \gg v$. For this ratio almost equal contributions of all electron-hole configurations to the exciton states S_i are found. There are only weak differences: for the two low-lying states the intradot arrangements dominate slightly over the interdot ones, while for the high-lying exciton states the interdot constituents are more important. As these variations are small, the peaks in Fig. 8 can be assumed to have the same heights.

Disregarding an overall phase for each state, the four exciton states in increasing order of energy can therefore be approximated by

$$|S_1\rangle \propto |0,0\rangle + |1,1\rangle + |0,1\rangle + |1,0\rangle,$$

$$|S_2\rangle \propto |0,0\rangle - |1,1\rangle - |0,1\rangle + |1,0\rangle,$$

$$|S_3\rangle \propto |0,0\rangle - |1,1\rangle + |0,1\rangle - |1,0\rangle,$$

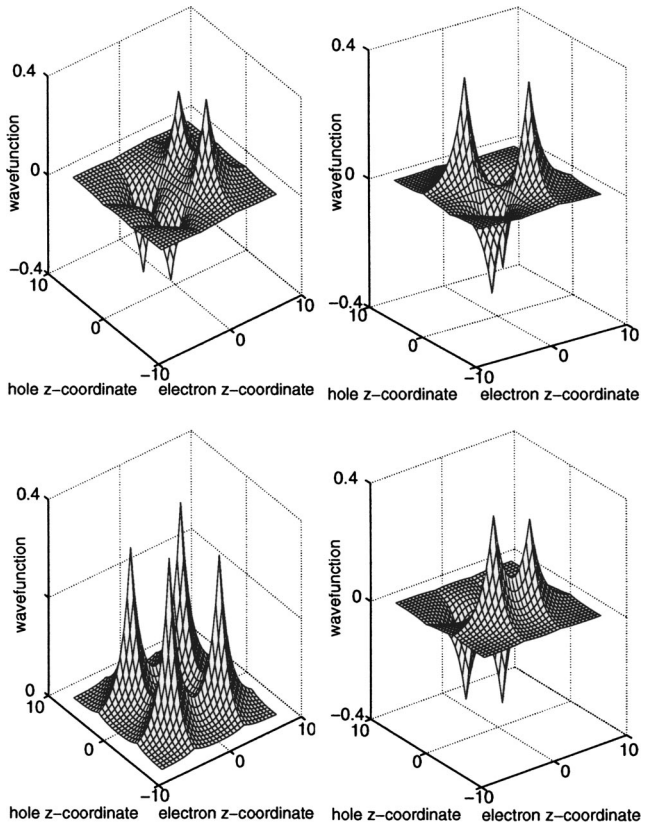

FIG. 8. Contour plots of the normalized exciton wave functions of the four lowest-lying exciton states in a highly symmetric quantum dot molecule consisting of two identical dot structures separated by a 5-nm-wide barrier. The lower left (right) panel shows $|S_1\rangle(|S_2\rangle)$ while the upper left (right) panels shows $|S_3\rangle(|S_4\rangle)$. Shown is the amplitude of the wave function as function of the electron and hole coordinates along the molecule axis. Note that the *z*-axis ranges are different in the different panels.

$$|S_4\rangle \propto |0,0\rangle + |1,1\rangle - |0,1\rangle - |1,0\rangle. \tag{2}$$

When setting the electron and hole coordinates equal ($\mathbf{r}_e = \mathbf{r}_h$), the states can be characterized by their symmetry along the molecule axis: the two energetically outer-lying states have even symmetry, while the two middle states have odd symmetry. This can be nicely seen from the wave functions in Fig. 8: the condition of equal electron and hole coordinates ($z_e = z_h$) is fulfilled for the in-plane diagonal running from $(z_e, z_h) = (-10, -10)$ to $(+10, +10)$. Evidently $|S_1\rangle$ and $|S_4\rangle$ are symmetric; $|S_2\rangle$ and $|S_3\rangle$, on the other hand, are antisymmetric.

These symmetry properties are independent of barrier width for molecules that are invariant under reflections at $z = 0$. They have drastic consequences for the optical activities of the exciton states: the oscillator strength is given by the probability of finding electron and hole at the same position. For its calculation the corresponding exciton amplitudes have to be summed: in each of the states the two intradot configurations $|0,0\rangle$ and $|1,1\rangle$ have equal amplitudes, as expected from the inversion symmetry. The sum of wave function amplitudes therefore vanishes for the antisymmetric states $|S_2\rangle$ and $|S_3\rangle$, which are consequently optically inactive, while the symmetric states $|S_1\rangle$ and $|S_4\rangle$ are optically active. The two strong emission lines that were observed experimentally for single molecules in Ref. 14 in the energy range of the *s* shell were accordingly attributed to the optically active states $|S_1\rangle$ and $|S_4\rangle$ there. Vice versa, from the observation that the spectra are dominated by two lines only, it can be concluded that the structures have rather high symmetry.

One further remark on the approximate forms in Eqs. (2): as discussed, from the configurations in Fig. 8 one notes that the weights of states $|0,0\rangle$ and $|1,1\rangle$ are slightly larger than those of the two interdot configurations $|0,1\rangle$ and $|1,0\rangle$. For the ground state $|S_1\rangle$, for example, these weights are ~ 0.36 and 0.31, respectively. It is actually important that the weights of the single particle configurations differ slightly in amplitude for the arguments that have been used in Ref. 14 to establish a relation of the pair states of electron and hole in the molecules to quantum information processing. At first sight, the wave function forms seemingly represent entangled states of an electron and a hole. However, one has to check carefully whether the particular choice of a representational basis just mimics entanglement despite of its absence, or in other words, if there is entanglement it has to be basis independent.

To obtain the above representations, we have used a localized basis formed by single particle states in which electron and hole are confined in one of the two dots or in opposite dots. However, when using the delocalized basis of bonding and antibonding molecules orbitals $|B\rangle_j / |AB\rangle_j = (|0\rangle_j \pm |1\rangle_j)/\sqrt{2}$, $j = e, h$, the first state $|S_1\rangle$ in Eqs. (2) can be simply written as product of the bonding electron and the bonding hole state $|S_1\rangle = |B\rangle_e |B\rangle_h$. Similarly also the three other states can be expressed as pure product forms. Obviously the states $|S_i\rangle$ would not be entangled then. The slight weight differences of the single particle configurations ensure that the entanglement does not break down under basis change.

In Ref. 30 we have shown for slightly different molecule parameters that the energy splitting between the states $|S_1\rangle$ and $|S_4\rangle$ increases strongly with decreasing barrier width. For completeness this dependence is shown again for the present case in Fig. 9 and discussed in greater detail in the following. The energies of the optically active states are given by the solid lines; those of the optically inactive states by the dotted lines. The widths of the lines give the relative oscillator strengths of the two optically active states.

First the barrier width dependence of the energies will be discussed: the exciton states arrange themselves in doublets. States $|S_1\rangle$ and $|S_2\rangle$ as well as $|S_3\rangle$ and $|S_4\rangle$ are located rather close in energy for all barrier widths. The splitting between these doublets, on the other hand, may exceed more than 50 meV for narrow barriers (considerably larger than what is seen in experiment). In this range it is determined by the tunneling matrix elements, mostly of the electron due to its small mass. For wide barriers, on the other hand, there is still a splitting of the states by about 10 meV, even though the single particle tunneling splittings tend to zero. This difference results from the Coulomb interaction, which dominates over the tunneling for large *d*. As will be shown below, the

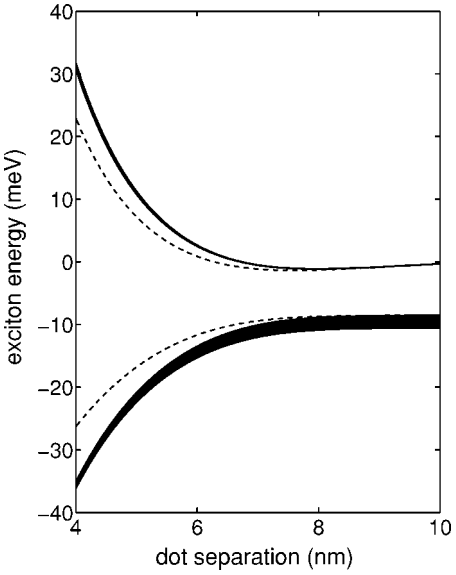

FIG. 9. Relative energies of the four exciton states that arise from tunnel splitting of a quantum dot *s*-shell ground state exciton versus the width of the barrier in a molecule structure of high symmetry. The solid (dotted) lines are for the two optically active (inactive) states. The linewidths indicate the oscillator strengths of the exciton transitions. The material parameters used for these calculations are given in the text. The energies are given relative to the energy of an exciton consisting of an electron and a hole in adjacent quantum dots with very large separation. The Coulomb correlation vanishes for this exciton complex. The energies of states $|S_1\rangle$ and $|S_2\rangle$ are lowered relative to this reference energy by the exciton binding energy. Exciton fine structure effects are not included in the calculations.

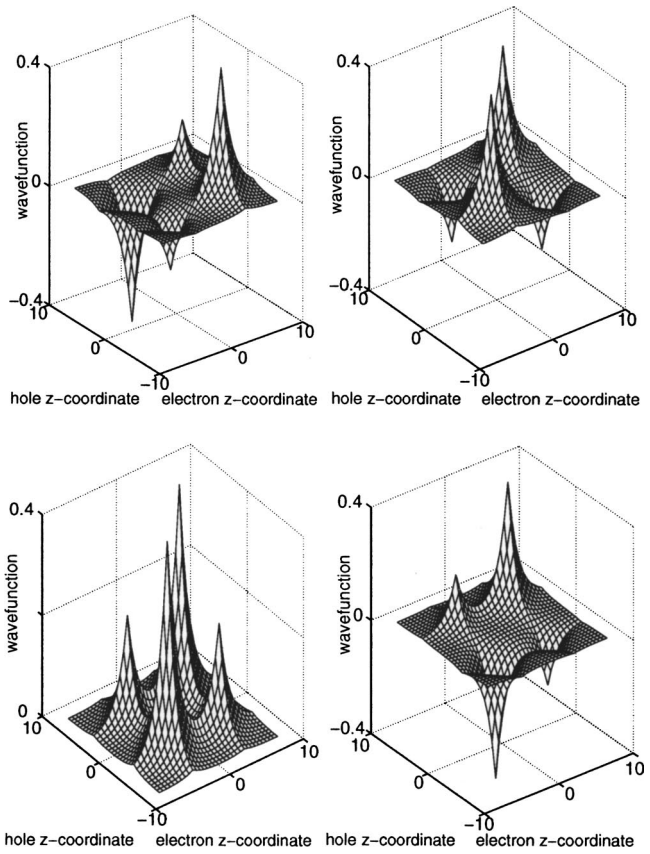

FIG. 10. Contour plots of the normalized exciton wave functions of the four lowest-lying exciton states in a highly symmetric quantum dot molecule consisting of two identical dot structures separated by a 7-nm-wide barrier. The lower left (right) panel shows $|S_1\rangle(|S_2\rangle)$ while the upper left (right) panels shows $|S_3\rangle(|S_4\rangle)$. Shown is the amplitude of the wave function as a function of the electron and hole coordinates along the molecule axis.

two lower states consist mostly of intradot electron-hole configurations, while the upper states are formed dominantly by interdot configurations. For the latter the electron-hole interaction goes to zero, because electron and hole are widely separated from each other for large d, while for the former the interaction energy approaches the exciton binding energy in an isolated dot. The energy splitting in the limit of wide barriers is therefore just given by the electron-hole interaction energy.

From the barrier width dependence we can thus conclude that to some extent the picture of bonding and antibonding states with even and odd symmetry along the molecule axis that comes from a single particle picture can be maintained also for excitons. States $|S_1\rangle$ and $|S_4\rangle$ represent the excitonic analogs of bonding and antibonding levels which repel each other in energy for increasing dot coupling, even though their symmetry properties are very much different from those of the single particle states, as both are symmetric along the molecule for $\mathbf{r}_e=\mathbf{r}_h$. Still we will term them here "bonding" and "antibonding" exciton states, for simplicity.

We turn to the oscillator strengths, which are about equal for the two optically active states in the narrow barrier molecules. With increasing d, however, oscillator strength is transferred from $|S_4\rangle$ to $|S_1\rangle$, until the ground state exciton oscillator strength is by far larger than that of the excited state for the wide barrier structures. Along the line of the previous discussion, this barrier width behavior originates from variation of the ratio of tunneling and Coulomb interaction: for the narrow barrier samples, due to the dominance of the tunnel coupling over the Coulomb interaction, intradot and interdot excitons contribute approximately with equal strengths to the wave function forms, as demonstrated for the excitons in the $d=5$ nm sample. From the approximate forms in Eqs. (2) one directly obtains equal oscillator strengths for the two optically active states. On the other hand, for the wide barrier samples, the Coulomb interaction dominates the tunnel coupling, leading to a strong change of the mixing of the single particle configurations. The two low-energy excitons are then mainly composed of intradot excitons, and it is their symmetry that makes $|S_1\rangle$ and $|S_2\rangle$ optically active and inactive, respectively. The two high-energy states, on the other hand, contain strong interdot exciton components, with the corresponding consequences for the oscillator strengths of $|S_3\rangle$ and $|S_4\rangle$.

This can be seen from the wave functions for a 7 nm barrier sample of high symmetry, shown in Fig. 10. The weight of the intradot configurations in state $|S_1\rangle$ is about 0.4, while that for the interdot configurations is roughly 0.2 only. In addition to the negative amplitude of the interdot states, for state $|S_4\rangle$ the basic change as compared to $|S_1\rangle$ is an

exchange of weights between direct and indirect excitons. Consequently the ratio of oscillator strengths of $|S_1\rangle$ and $|S_4\rangle$ is roughly 4:1 for a 7 nm barrier, and the ratio becomes even larger for wider barriers.

Each of the states $|S_i\rangle$ represents a fine structure multiplet consisting of four levels, according to the number of different spin orientation configurations of electron and hole. It is the exchange interaction which couples these spins so that the exciton states can be characterized by a total angular momentum quantum number, if the rotational symmetry around the molecule axis is not broken. The exchange lifts the energetic spin degeneracy of the excitons, depending on the symmetry of the structure. The involved splitting energies are typically much smaller than those of the orbital states $|S_i\rangle$, except for very wide barriers (see discussion below).

For the situation of a molecule with unbroken rotational symmetry, the resulting eigenstates are the same as in a single quantum dot of rotational invariance. There are two spin-bright states with z component of the exciton angular momentum $M=\pm 1$, and two spin-dark states with $M=\pm 2$. The dark excitons are shifted to lower energies relative to the bright excitons due to the (long-range) exchange interaction. Bright and dark excitons form degenerate doublets (neglecting a tiny splitting of the $M=\pm 2$ states due to the short-range part of the exchange).[30] The effects of a symmetry reduction on the fine structure will be discussed in detail in Secs. IV and V. Deliberate insight into state degeneracies can be taken by applying a magnetic field B and thereby switching on the Zeeman interaction of carrier spins. Typically the spin splitting leads to a considerable enhancement of the energy splitting of the fine structure levels and thus facilitates their spectroscopic resolution.

With these considerations the picture of exciton states in molecule structures that originate from the ground state exciton in the isolated dots can be completed: the total number of states is 16, resulting from the four different possibilities of spatial carrier distribution in a double dot system (leading to the states $|S_i\rangle$) times the different spin configurations for each of these states.

The model for the orbital exciton states up to this point does not capture perturbations of the symmetry of the molecule structure, due to which all four states $|S_i\rangle$ might become optically active. Asymmetries also will cause the exciton angular momentum being no longer a good quantum number and will lift spin degeneracies because spin-bright and - dark states will become mixed. In effect, all the 16 available states could contribute to the s-shell emission of a molecule structure. The origin of such a symmetry breaking could lie in a deliberate breaking by application of external electromagnetic fields or could be structure inherent. For example, the quantum dots could be different or could be laterally (in the molecule plane) displaced with respect to each other. A symmetry breaking is also expected if the dots are not disk shaped but if they are dome or pyramid shaped, which obviously leads to a lack of inversion symmetry along the molecule axis. For self-assembled molecule structures most likely the complicated strain distribution around the dots will break the symmetry anyway, independent of the dot shape.[18] However, the strength and effect of this symmetry lowering are not clear yet, as no detailed relation between experimental data and microscopic details of the structures can be made. The impact of strain, for example, may be weakened by intermixing of dot and barrier material.

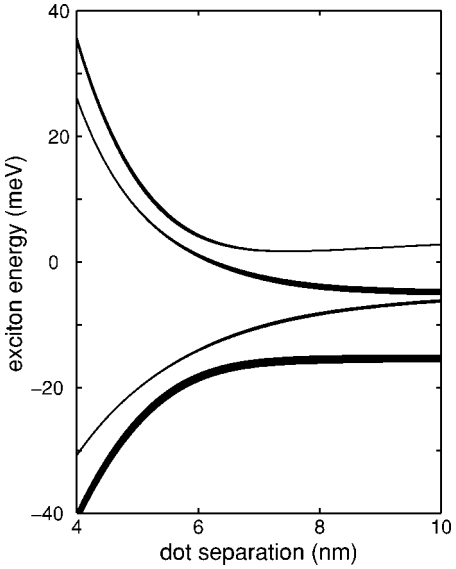

FIG. 11. Energies of the four exciton states that arise from tunnel splitting of a quantum dot s-shell exciton versus the width of the barrier in a molecule structure of strongly reduced symmetry (see text for parameters). Since all four exciton states are optically active, only solid lines have been used for presentation, in contrast to Fig. 9. The linewidths indicate the oscillator strengths of the exciton transitions. As in Fig. 9, the energies are given relative to the energy of an exciton formed by an electron and a hole in adjacent, widely separated quantum dots of a highly symmetric molecule. Exciton fine structure effects are not included in the calculations.

To capture the effects of deviations from an ideal structure on a more quantitative level, Fig. 11 shows the barrier width dependence of the exciton energies in a strongly "perturbed" molecule structure consisting of two considerably different quantum dots (no lateral displacement).[30] To account for the asymmetry, their confinement potentials were assumed to differ by 15 meV for the electrons and by 3 meV for the holes, corresponding to a few percent variation of the potential heights. The used set of material parameters is as follows. For the electron (hole) potential heights we use 680 and 665 meV (100 and 97 meV). For the carrier masses we have used the same values as given above for the symmetric structure.

The consequences of the assumed asymmetry are the following. First, an increase of the splitting between the exciton states is clearly seen as compared to the symmetric structure. This increase concerns first the splitting among the two state doublets $|S_1\rangle$ and $|S_2\rangle$ as well as $|S_3\rangle$ and $|S_4\rangle$: For a 6 nm barrier width we find, for example, a splitting of $\sim$25 meV between $|S_1\rangle$ and $|S_4\rangle$ in the asymmetric structure, while it is only $\sim$20 meV for the symmetric molecule. Second, also the splitting between the states in a doublet is very much enlarged for this particular choice of molecule asymmetry. For wide barriers, the energies of states $|S_2\rangle$ and $|S_3\rangle$ tend to converge and are located roughly in the middle between the two outer states $|S_1\rangle$ and $|S_4\rangle$.

The origin of the overall increase of energy splitting may be understood in a single particle picture: for a symmetric quantum dot molecule the coupling of electron states is described by a 2×2 matrix

$$\begin{pmatrix} E_e & t_e \\ t_e & E_e \end{pmatrix}, \tag{3}$$

where we have used again the basis of localized states $|0\rangle$ and $|1\rangle$ for matrix representation. E_e is the energy of the electron in a decoupled dot and t_e is the tunneling matrix element. Diagonalizing this matrix by going from the basis of localized states to that of delocalized(bonding and antibonding) states $(|0\rangle_e \pm |1\rangle_e)/\sqrt{2}$ gives the eigenenergies $E_e \pm t_e$.

For an asymmetric structure the electron energies E_e are different, so that the matrix is given by

$$\begin{pmatrix} E_{e,1} & t_e \\ t_e & E_{e,2} \end{pmatrix} \tag{4}$$

with $E_{e,1} \neq E_{e,2}$. Calculations show that the modification of the tunneling matrix element by the asymmetry is rather small, as long as the asymmetry is not too large, as would be the case for strongly laterally displaced dot structures. Diagonalization gives eigenenergies, the splitting of which is enlarged as compared to that for the symmetric molecule structure by the energy difference between the two electron states:

$$E_{1,2} = \frac{1}{2}(E_{e,1} + E_{e,2}) \pm \frac{1}{2}\sqrt{4t^2 + (E_{e,1} - E_{e,2})^2}. \tag{5}$$

For an exciton the increase of level splitting will be renormalized by the effects of the Coulomb interactions between electron and hole.

The asymmetry also leads to a mixing of the optically active and inactive states making the latter ones observable. Figure 12 shows contour plots of the four *s*-shell exciton states $|S_1\rangle$ to $|S_4\rangle$, in analogy to those shown for the highly symmetric molecule in Fig. 10. The barrier width again is 7 nm. The states can no longer be categorized according to their symmetry properties along the molecule axis (i.e., the in-plane diagonal $z_e = z_h$), reflecting directly the loss of inversion symmetry. When calculating the exciton oscillator strength, for which we have to consider the wave function amplitudes along this diagonal, we find for all states finite values making them optically active.

Moreover, the spatial distribution of the exciton states has strongly changed. For the ground state $|S_1\rangle$ the electron and hole are predominantly localized in one dot, and form mostly an intradot exciton $|0,0\rangle$, with rather weak admixtures from the other single particle configurations. The state $|S_2\rangle$ on the other hand has gained a strong interdot exciton character, but it still has a significant intradot $|1,1\rangle$ component as well. The state $|S_3\rangle$ has comparable intradot and interdot components similar to $|S_2\rangle$, while it was optically inactive for the structure of high symmetry. Finally, the formerly bright state $|S_4\rangle$ has even become a predominantly indirect state due to the symmetry reduction.

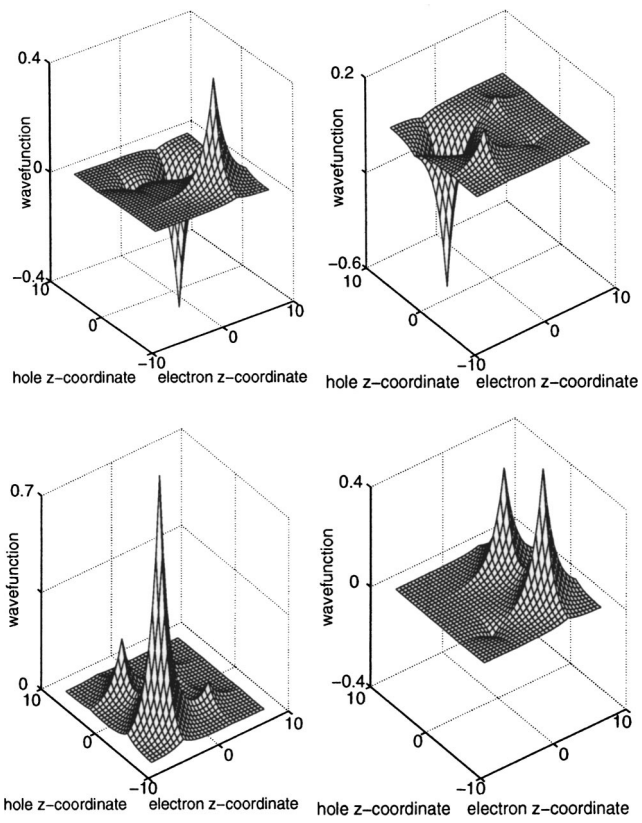

FIG. 12. Contour plots of the normalized exciton wave functions of the four lowest-lying exciton states in a highly asymmetric quantum dot molecule consisting of two dot structures separated by a 7-nm-wide barrier (no lateral displacement). The electron confinement potentials differ by 15 meV, and those of the holes by 3 meV. The lower left (right) panel shows $|S_1\rangle(|S_2\rangle)$ while the upper left (right) panel shows $|S_3\rangle(|S_4\rangle)$. Shown is the amplitude of the wave function as function of the electron and hole coordinates along the molecule axis. Note that mostly the electron is affected by the wave-function redistribution caused by the molecule asymmetry.

From the very different spatial characters as compared to the high-symmetry case, more detailed insight into the energy splitting of the states for wide barriers ($v \gg t$) can be taken. Since the carriers tend to become localized in one of the dot structures for the wide barrier case, the electron-hole interaction is increased. This is compensated for by the corresponding increase of the kinetic energy. Taking into account also the effects of the dot asymmetry, the splitting between $|S_1\rangle$ and $|S_4\rangle$ is about twice as large as for identical dots. Strong changes occur also for states $|S_2\rangle$ and $|S_3\rangle$, which in the case of high symmetry are dominantly intradot and interdot, respectively. Through the symmetry breaking they obtain considerable admixtures of the complementary spatial distribution with the corresponding change of electron-hole interaction, so that in one case ($|S_2\rangle$) the energy is effectively increased, while in the other case ($|S_3\rangle$) the energy is effectively lowered. As a consequence their energies tend to converge for wide barriers.

When reducing the barrier width, the energy splitting among the four exciton states becomes more similar to the high-symmetry case. This is caused by the dominance of the

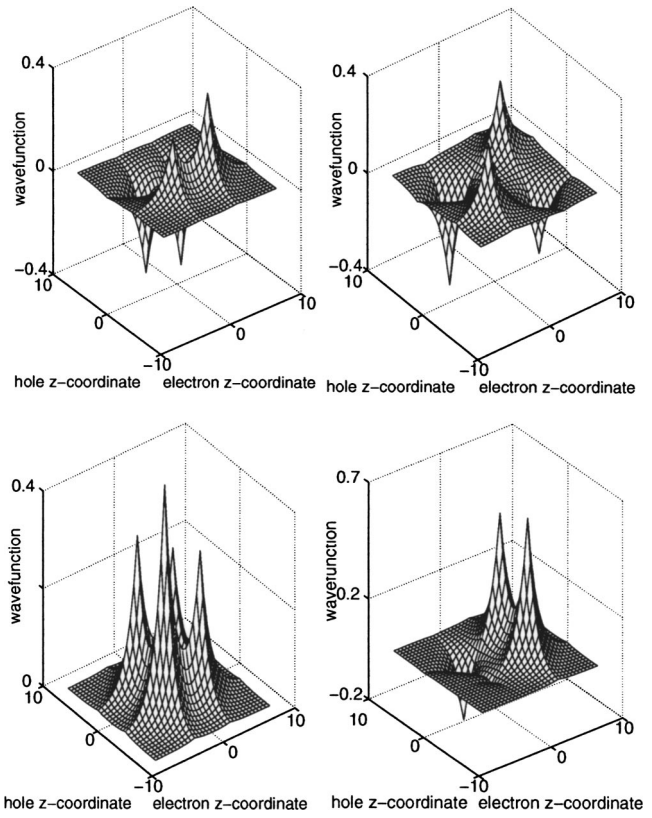

FIG. 13. Contour plots of the normalized exciton wave functions of the four lowest-lying exciton states in a highly asymmetric quantum dot molecule consisting of two dot structures which are separated by a 5-nm-wide barrier (no lateral displacement). The electron confinement potentials differ by 15 meV, and those of the holes by 3 meV. The lower left (right) panel gives $|S_1\rangle(|S_2\rangle)$ while the upper left (right) panel gives $|S_3\rangle(|S_4\rangle)$.

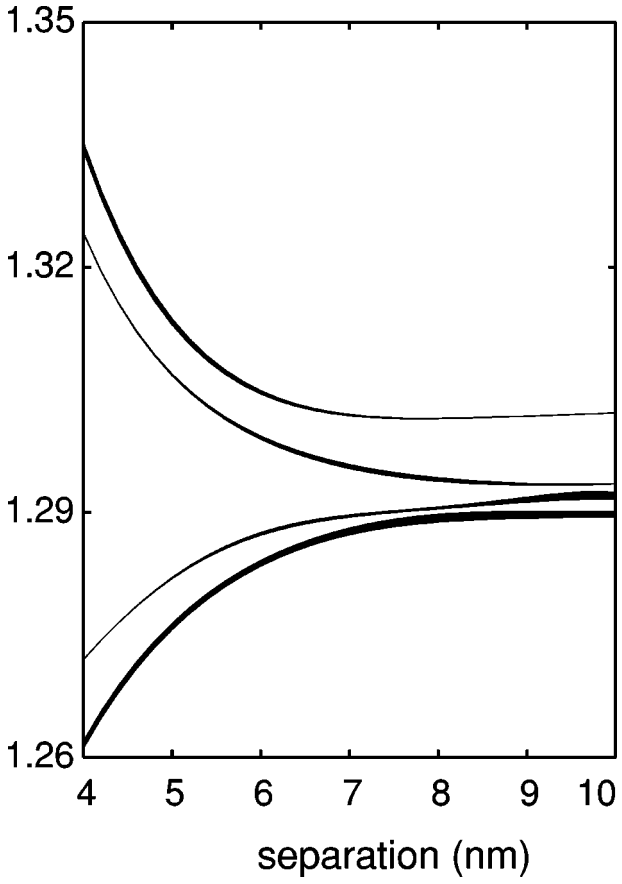

FIG. 14. Energies of the four exciton states that arise from tunnel splitting of a quantum dot *s*-shell ground state exciton versus the width of the barrier in a molecule structure of reduced symmetry: it consists of nonidentical dots that are laterally displaced by 4 nm, but the dot parameters are more similar to each other than those in Fig. 11 (see text for details). The linewidths indicate the oscillator strength of the exciton transitions. As in Fig. 9, the energies are given relative to the energy of an exciton formed by an electron and a hole in adjacent, widely separated quantum dots of a highly symmetric molecule. Exciton fine structure effects are not included in the calculations.

tunneling splitting over the Coulomb interactions ($v \ll t$), due to which the possibilities for spatial carrier redistributions within the molecule become restricted. This is confirmed by the wave functions of the four exciton states, that are shown in Fig. 13. The ground state is clearly delocalized over the molecule structure, but still the configuration $|0,0\rangle$ is slightly more important as compared to the $|1,1\rangle$ configuration. Similarly the carrier distributions in the excited states rather closely approach the high-symmetry situation. The reduced influence of derangement is also reflected by the redistribution of oscillator strength from $|S_3\rangle$ to $|S_4\rangle$ which occurs as soon as the hole tunneling becomes comparable to the asymmetry in energies.

As described in Ref. 19, asymmetry might be introduced not only by a difference of the dot structures but also through an (additional) lateral displacement of the dots relative to each other.[34] From scanning electron microscopy we know that the magnitude of this displacement is less than 5 nm for the wide barrier samples. Based on the above set of parameters for nonidentical dots we have checked the sensitivity of the exciton states with respect to such a derangement. We find it to be small for both energies and wave functions (not shown), as might be expected because lateral shifts by a few nanometers do not modify the tunneling probabilities of the carriers strongly, as would be the case for shifts above ~10 nm or more. A small displacement effectively increases the separation between dots slightly, so that the behavior for this situation is similar to that of a molecule with no displacement but slightly increased separation.

Irrespective of details of the calculations, a strong enough symmetry reduction will lead to optical activity of all four exciton states $|S_i\rangle$. We note, however, that the precise appearance of the molecule level splitting changes strongly with the strength of the symmetry breaking in the molecules. This is exemplified in Fig. 14 which shows the barrier width dependence of the exciton energies in a molecule composed of different dots that are additionally laterally displaced by 4 nm but differ by 2 meV only in the sum of electron and hole confinement potentials, clearly less than in the previous case. The parameters are identical to those used in Ref. 19: for demonstration of the dependence on structural details, we assume pure InAs in the dots giving an electron mass of 0.03, while for the other mass parameters the same values are

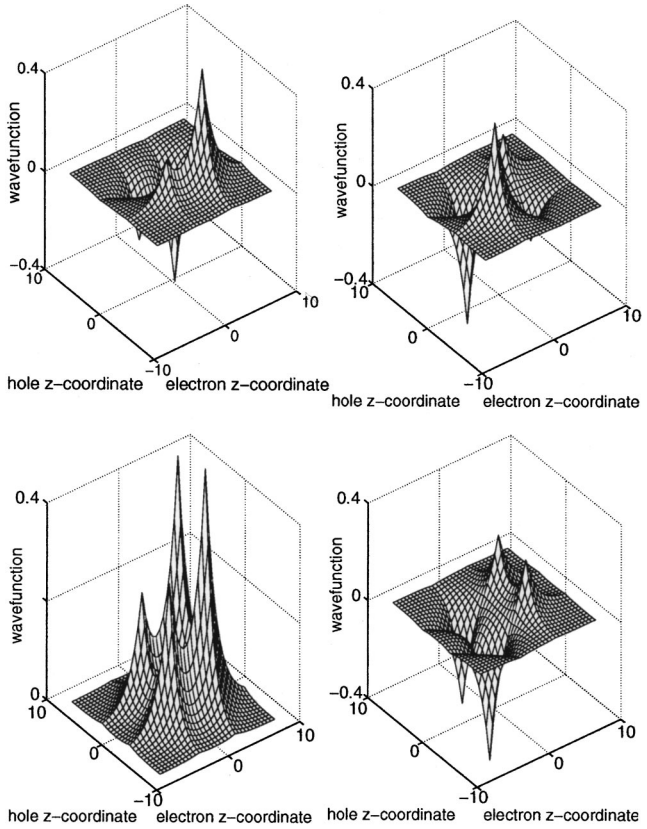

FIG. 15. Contour plots of the normalized exciton wave functions of the four lowest-lying exciton states in an asymmetric quantum dot molecule consisting of two dot structures which are laterally displaced by 4 nm and separated by a 5-nm-wide barrier. Further, the sum of the electron and hole lateral confinement potentials differ by 2 meV (see text for detailed parameter list). The lower left (right) panel gives $|S_1\rangle(|S_2\rangle)$, while the upper left (right) panel gives $|S_3\rangle(|S_4\rangle)$.

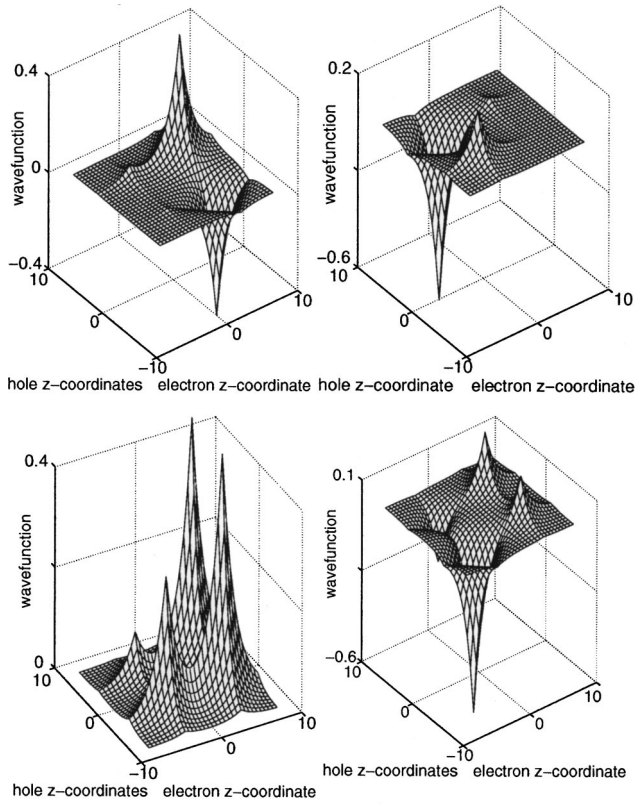

FIG. 16. Contour plots of the normalized exciton wave functions of the exciton states in an asymmetric quantum dot molecule consisting of two dot structures which are laterally displaced by 4 nm and separated by a 7-nm-wide barrier (for details see text). The lower left (right) panel gives $|S_1\rangle(|S_2\rangle)$ while the upper left (right) panel gives $|S_3\rangle(|S_4\rangle)$.

used as above. The potential offsets between InAs and GaAs are taken to be 600 (100) meV for electrons (holes).

The dot asymmetry of this structure in effect is reduced as compared to the case just discussed. Therefore the appearance of the energy versus separation graph is more similar to the high symmetry case: the splitting among exciton states is reduced. In particular, states $|S_1\rangle$ and $|S_2\rangle$ are located very close to each other. A closer look reveals even slight oscillations of their splitting which arise from the dependence of the matrix elements on the angle between the growth axis and the axis joining the two dots. This angle obviously varies as the dot separation is changed. The wave functions both for the 7 and 5 nm barriers in Figs. 15 and 16 demonstrate again the determining influence of the ratio of tunnel coupling t and Coulomb interaction v on the carrier distribution. For 5 nm all states are basically delocalized over the molecule structure; for the 7 nm barrier localization of carriers in one of the dots starts to play some role. Due to the asymmetry-induced mixing of the "ideal" exciton states all of them are optically active.

The activation of $|S_2\rangle$ and $|S_3\rangle$ through asymmetry-induced mixing with $|S_1\rangle$ and $|S_4\rangle$ might offer an explanation for the observation of more than two emission lines in some of the small mesa structures. An example is given in Fig. 17 showing an emission spectrum recorded on a 100-nm-wide mesa structure of the 8 nm barrier quantum dot molecule sample. For it, four emission lines are observed in the *s*-shell energy range, two of strong and two of weak intensity. One

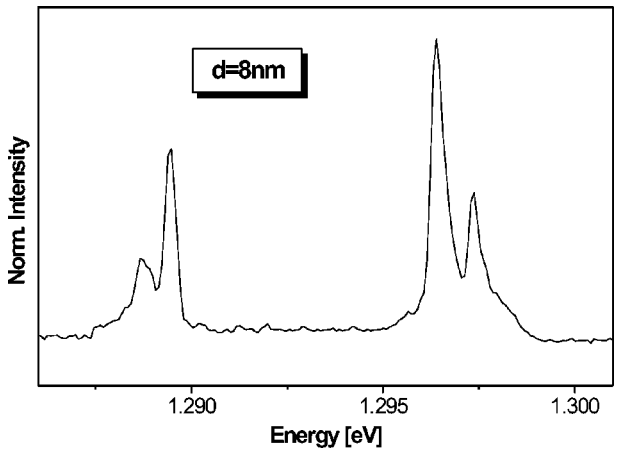

FIG. 17. Photoluminescence spectrum recorded on a 100-nm-wide mesa structure patterned on the quantum dot molecule sample with an 8 nm barrier ($T=10$ K). The excitation power density was 50 W cm^{-2}.

might argue that it is the reduced symmetry that in this case leads to optical activity of all the exciton states constructed above, but clearly such an interpretation would go too far: From photoluminescence experiments we cannot exclude the possibility that these lines do not come from one molecule only, but from two molecules, for example. Therefore a relation between the increased number of lines and the dot symmetry cannot be made. Such a relation might be established, however, in correlation measurements by which it can be ensured that all the lines indeed originate from a single quantum emitter.

V. SPECTROSCOPIC DATA AND DISCUSSION

The rather general discussion of the exciton states in coupled quantum dots in the previous section will serve in the following as basis and guide for understanding and interpreting the experimental results on the exciton fine structure.

A. Fine structure in the "bonding" exciton energy range for wide barrier samples

At a first view, the electronic coupling of the double dot structures by tunneling seems mostly under question for the structures with the widest barriers of 7 and 8 nm. For these samples photoluminescence studies, however, showed a splitting of the *s*-shell emission (see Figs. 2–4). A validation of the assignment of the observed spectral lines to recombination from excitons with wave functions that are extended over the molecule structure was provided by detailed investigations of the magnetic field dispersion of their fine structure. As frame for discussion we use the characteristic behaviors of the five different quantum dot molecules presented in Ref. 19 (labeled QDM1 up to QDM5 there). We will detail these data further and present a variety of additional results here. From the calculations for these wide barrier samples a rather small energy splitting between $|S_1\rangle$ and $|S_2\rangle$ on the order of 1 meV is expected, as long as the symmetry of the particular geometry is not broken too strongly. This splitting is small enough to induce resonances between several of the fine structure states of $|S_1\rangle$ and $|S_2\rangle$ when applying a magnetic field that is leading to their spin splitting. In the following we focus on the corresponding energy range.

At zero field for QDM1 up to QDM4 a single emission feature is observed, while QDM5 shows two closely spaced emission lines to be discussed further below. For QDM1 and QDM2 the spectral width of this feature is so small that it can safely be attributed to a single emission line. This indicates that any potential symmetry breaking is not strong enough that $|S_2\rangle$ obtains enough oscillator strength so that it can be observed in experiment and only $|S_1\rangle$ contributes to the emission. For QDM3 and QDM4 the linewidth of the $B=0$ spectral feature is considerably larger. Moreover, the emission intensity is slightly modulated, so that apparently a few optical transitions contribute to the luminescence. From the data the precise number of involved transitions is, however, hard to assess. Through the modulations their number can be estimated to be 2–3.

The clearest picture for a quantum mechanically coherent coupling of the molecule quantum dots has been obtained for

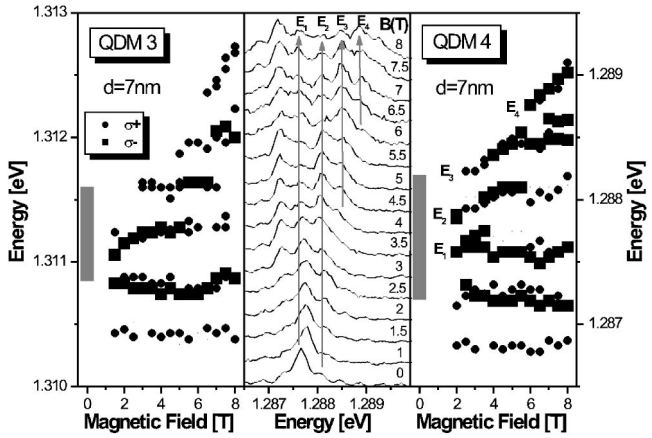

FIG. 18. The left panel gives the magnetic field dispersion of the *s*-shell exciton transition energies of QDM3 in Ref. 19. The field was applied in the Faraday configuration. The middle panel shows photoluminescence spectra of QDM4 of Ref. 19 at different magnetic fields. The lines are guides to the eye, to follow the different transitions labeled E_i, $i=1,\ldots,4$. The right panel gives the resulting field dispersion of the transition energies for QDM4. Both structures had a barrier of 7 nm nominal width. For the left and right panels polarized spectra have been used to determine the transition energies with higher precision. The types of symbols give the energies in the different polarizations. The bars at zero magnetic field indicate the base widths of the $B=0$ emission lines. The sizes of the symbols give the relative intensities of the lines.

QDM3 and QDM4. The middle panel of Fig. 18 shows photoluminescence emission spectra of QDM4 for different magnetic fields in the Faraday configuration. The zero-field emission band is rather broad with a base linewidth of about 1 meV. In magnetic field it splits into a multiplet of spectral lines consisting of up to seven distinguishable features. From this number of lines it is clear that not only a single quantum dot is addressed, for which a splitting into not more than four lines could occur. Instead, two dots must be involved (at least). If the two dots were decoupled, two emission lines at different energies would be observed at $B=0$, since an energetic coincidence is practically excluded, as it would require virtually identical quantum dots. Moreover, in magnetic field the two lines would split into two independent fine structure multiplets, that is, whenever two states belonging to the different multiplets come into resonance, they would cross each other without interaction, as seen for the 16 nm barrier molecule. For clarity, this has been sketched in Fig. 19.

Instead, for QDM3 and QDM4 several sequential anticrossings at different magnetic fields are observed. The avoided crossing processes are evidenced most clearly by a redistribution of emission intensity (oscillator strength) among lines, as shown exemplarily for the features labeled E_1, E_2, E_3, and E_4 in the spectra of QDM4 in Fig. 18. Below $B=3$ T, E_1 is the dominant spectral line, E_2 appears only at about 2 T, and E_3 as well as E_4 cannot be seen at all. When ramping B up to 5 T, the E_1 intensity decreases and E_2 becomes the dominant feature in the spectrum. Simultaneously E_3 emerges on the high-energy side. Between 5 and 7 T the lines E_2 and E_3 undergo a qualitatively similar exchange of emission intensity as seen before for the E_1 and E_2 doublet.

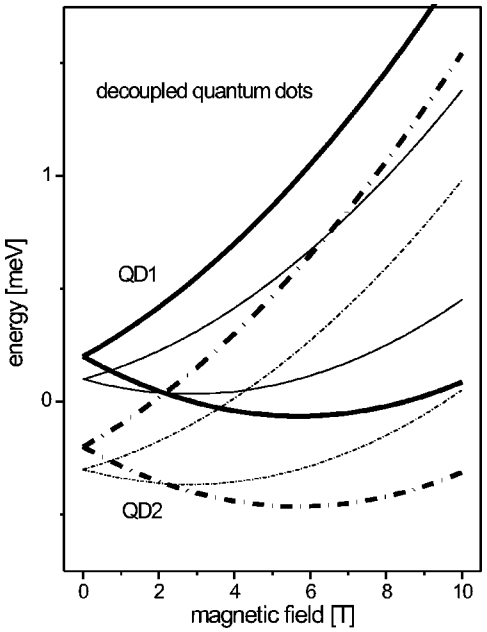

FIG. 19. Scheme of the exciton fine structure of two independent quantum dots QD1 and QD2 of high symmetry. Thick (thin) solid lines correspond to bright (dark) exciton states of QD1. The dash-dotted lines do the same for QD2. For both dots the same fine structure parameters were used. For the diamagnetic shift we assumed a B^2 form with a coefficient 8.2 μeV/T^2 for both bright and dark excitons. The B-linear spin splitting was 0.093 meV/T for the bright excitons, and 0.046 meV/T for the dark excitons. For the exchange energy splitting of bright and dark excitons we use 100 μeV. These parameter choices rely on typical data from the quantum dot reference sample.

Another such exchange between E_3 and E_4 takes place at the highest applicable field strengths. There a further line emerges on the high-energy side. The orbital molecule states $|S_1\rangle$ and $|S_2\rangle$ provide a sufficient number of fine structure states to account for the number of features in the experiment.

For clarity we note that the emission intensities of the different transitions, whose relative strengths are indicated by the sizes of the symbols in Fig. 18, obviously do not correspond directly to the oscillator strengths of the involved states. Due to the nonresonant continuous wave laser excitation the crystal temperature might not correspond to the bath temperature, although the illumination power is kept as small as possible to still obtain a reasonable signal-to-noise ratio. The photogenerated carriers relax toward the molecule ground states by phonon emission, "heating up" the crystal. Despite the immersion in superfluid helium there might be some remaining effect of this relaxation. For a cautious estimate we assume a sample temperature of 10 K, corresponding to a thermal energy k_BT of about 1 meV. k_BT has thus about the same magnitude as the energy range over which the fine structure effects occur. Still, thermal equidistribution of carriers within the fine structure multiplet cannot be assumed as this would require thermal energies much larger than the energy splitting between the different states. Only under this condition would the emission intensities directly reflect the oscillator strengths within the whole multiplet.

How carriers become distributed among the fine structure levels, each of which represents a certain spin configuration, cannot be assessed from the present data. As the excitation was done above the GaAs barriers, one can assume that carriers become fully depolarized before relaxation, since the spin-flip times are rather short in higher-dimensional systems, in particular for the holes.[35] The relaxation within the fine structure multiplet is determined by acoustic phonon absorption and emission processes (which are rather slow on the time scale of radiative recombination), also involving spin flips. Precise knowledge about these processes has to be developed yet. Still close to the anticrossing points the splitting between the two states that repel each other is so small (less than 0.5 meV in each case) that the emission intensities to a good approximation reflect the oscillator strengths of the levels that repel each other, for which they obviously need to have the same symmetry character. In particular, the hybridization leads to a similar spin configuration for them.

The avoided crossings can be seen also in the magnetic field dispersion of the transition energies for QDM4 in the right panel of Fig. 18, although this is hampered by the multiple number of states that become mixed. For example, E_3 shows a clear high-energy shift up to $B=5$ T, which is converted into a weak field dependence above 5 T. The high-energy shift is taken over by E_4. The anticrossings appear not as prominent as for QDM3, which shows at high fields a splitting into six features only (the left panel of Fig. 18). Here the anticrossing between the third and the fourth spectral lines around 4 T can be nicely seen, even though after anticrossing the high-energy line does not show a high-energy shift itself, but immediately comes into resonance with the next higher-lying line, with which it exchanges character as well. This line then continues the original shift to higher energies with increasing field. For QDM4 so many states are involved in level mixings that the avoided crossings are somewhat obscured in the frequency domain, but can be traced from the exchange of oscillator strength among them.

Anticrossings such as the observed ones can occur only if the two dot structures are quantum mechanically coherently coupled. For the underlying state mixings physical mechanisms are required that lead to a spin precession (without decoherence) through which different spin angular momentum states become coupled. The observations could be explained by a theoretical model from which the results were attributed to a lateral displacement of the quantum dots implying a symmetry breaking (see Refs. 19 and 30). This symmetry breaking "switches on" state mixings in magnetic field, for the origins of which the following interactions can be identified. For the hole states a mechanism is provided by the anisotropic Zeeman interaction arising from mixing of the Γ_8 and Γ_7 valence bands in the Kane Hamiltonian. Due to its anisotropy it acts like an in-plane magnetic field. For the electrons, on the other hand, a mechanism is provided by the intraband spin-orbit coupling. Using the above notation, these interactions lead to a hybridization of states within each of the $|S_1\rangle$ and $|S_2\rangle$ fine structure multiplets and also of states belonging to the two different multiplets.

Figure 20, left panel, gives photoluminescence spectra of another quantum dot molecule, different from QDM3 and

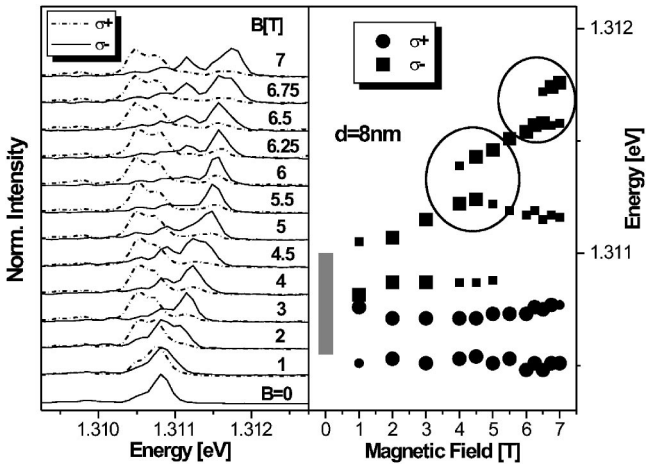

FIG. 20. Left panel: Circular-polarization-resolved photoluminescence spectra of an InAs/GaAs quantum dot molecule with an 8-nm-wide barrier for different magnetic fields (Faraday configuration). Right panel: The resulting exciton transition energies versus magnetic field. The bar at $B=0$ gives the base width of the zero-field emission feature. The types of symbols indicate the dominant polarization of the lines, their sizes give the relative emission intensities. The circles highlight anticrossing processes within the fine structure multiplet.

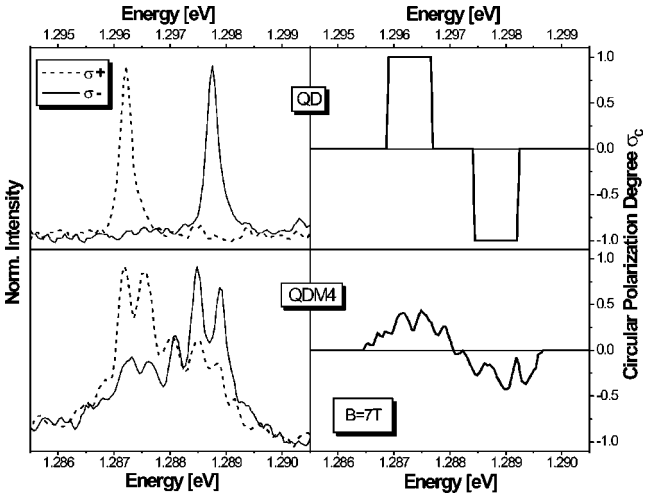

FIG. 21. Left panels: Circular-polarization-resolved photoluminescence spectra at $B=7$ T for a single quantum dot (upper left panel) and QDM4 of Ref. 19 with a 7-nm-wide barrier (lower left panel). Right panels: The resulting circular polarization degrees σ_C for the single dot (upper right panel) and for QDM4 (lower right panel) as a function of energy.

QDM4, with a barrier width of 8 nm. Its emission has been analyzed with respect to its circular polarization. The transition energies that were derived from these spectra are displayed in Fig. 20, right panel. Again distinct anticrossings are observed in the magnetic field dispersion (as indicated by the circles), although the details of these features are different from those for QDM3 and QDM4. In particular, at high magnetic fields only five features can be resolved. This demonstrates that the fine structure patterns depend strongly on the details of the molecule geometry, which itself varies from molecule to molecule. For completeness we state that we do not find significant differences in the fine structure for 7 and 8 nm barrier widths.

It is also interesting to look at the circular polarization degree σ_C of the emission. σ_C will be defined as the difference between the right and the left circularly polarized emission intensities, divided by the sum of the two, $\sigma_C = (I^+ - I^-)/(I^+ + I^-)$. For quantum dots, one typically observes at high magnetic fields two well separated emission lines which are either completely σ^+ or σ^- polarized, even for highly asymmetric dot structures, which show a linear polarization splitting at $B=0$. An example for single dot emission at $B=7$ T is shown in the upper left panel of Fig. 21, from which the full circular polarization is nicely seen. The linear zero-field polarization arises from the mixing of the $M=+1$ and $M=-1$ exciton states induced mostly by the long-range exchange interaction between electron and hole. However, moderate magnetic field strengths are sufficient to restore the circular polarization since the Zeeman interaction energy of the carrier spins at these field strengths typically is considerably larger than the electron-hole exchange energy. Therefore the polarization degree switches almost "digitally" from +1 to −1 when scanning over the energy range in which the emission doublet is located, as shown for the single dot in the upper right panel of Fig. 21. We point out that to calculate the circular polarization at energies where no dot emission is observed, the emission intensity has been set to zero. This has been done because the spectral noise in these energy ranges would lead to unphysical results for σ_C, such as $|\sigma_C| > 1$.

The behavior of the dot emission is in striking difference to the observations for QDM3 and QDM4. Figure 21, lower left panel, shows circularly polarized photoluminescence spectra of QDM4 at $B=7$ T, taken from Ref. 19, and the lower right panel shows the corresponding polarization degree versus energy. None of the spectral lines is completely circularly polarized, as is observed also for the quantum dot molecule in Fig. 20. Accordingly the polarization shows a comparatively smooth behavior superimposed by oscillations from the several emission lines in the spectrum: the polarization has extreme values at the energies of these lines, but the maximum σ_C is roughly 40% only. This clearly shows that in these structures the circular symmetry cannot be restored by a magnetic field, even for the highest available field strengths, since still significant state mixings occur there. The lateral displacement of the dots in the molecules naturally causes a much stiffer symmetry reduction of the electronic states than the asymmetry of a single quantum dot, which shows itself for the ground state exciton through the modification of the exciton exchange, which is small anyway. It thus can be easily overpowered by the considerably stronger Zeeman interaction of the carriers, resymmetrizing the carrier states. In the asymmetric molecules a corresponding redistribution of the wave function is not simply possible because the carriers are distributed over a nonsimply connected geometry.

This is in agreement with the theoretical model that we have developed in Ref. 30 (see below). We note, however, that from the calculations a full circular polarization of the emission is expected for magnetic field strengths at which

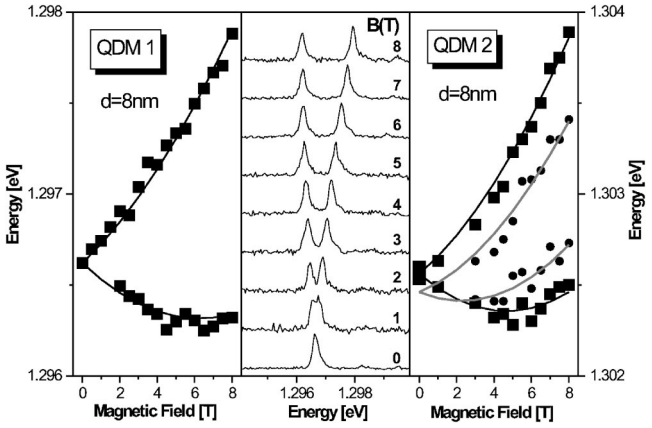

FIG. 22. The middle panel shows photoluminescence spectra of QDM1 of Ref. 19 recorded at different magnetic fields in the Faraday configuration. The left panel gives the resulting magnetic field dispersion of the transition energies for QDM1. The right panel gives the field dispersion of transition energies for the QDM2 in Ref. 19. The lines are fits to the data assuming a B-quadratic diamagnetic shift superimposed by a B-linear spin splitting. The black (gray) curves are for the spin-bright (spin-dark) exciton states.

the Zeeman interaction energy is so large that all fine structure levels are well separated from each other, so that they are no longer hybridized. From the data we would expect this to occur for fields well above 10 T, not available in present experiments.

Also the fine structure patterns of two other molecules, QDM1 and QDM2, which showed a splitting strongly reminiscent of that of a single quantum dot, were reported in Ref. 19. The middle panel of Fig. 22 shows the emission spectra of QDM1 for different magnetic fields in the Faraday configuration. The narrow zero-field emission line shows a doublet splitting, which continuously increases, when the magnetic field is ramped, as seen from the B dependence of the transition energies in the left panel. It depends linearly on magnetic field and reaches 1.5 meV at $B=8$ T. The right panel gives the field dispersion of the transition energies of QDM2. For it, the emission is also dominated by a doublet. In between two additional spectral features of weaker intensities appear, which we attribute to "dark" exciton recombination. By "dark" we refer here not to the spatial distribution of the wave function but to configurations of the electron and hole spins, which lead to exciton angular momenta $M=\pm 2$. As mentioned, these splitting patterns of QDM1 and QDM2 do not distinguish these structures from a single quantum dot.

To understand whether the QDM1 and QDM2 emissions come from a single dot or from a quantum dot molecule, we have measured the exciton diamagnetic shift with the field applied normal to the heterostructure growth direction (taken as the z direction). This shift is a measure for the extension of the exciton wave function along the molecule axis: assuming a magnetic field orientation parallel to the y axis ($\mathbf{B}=\mathrm{rot}\,\mathbf{A}=B\mathbf{e}_y$) we can use the gauge $\mathbf{A}=B\cdot z\mathbf{e}_x$ for the vector potential, where the $\mathbf{e}_i$, $i=x,y$, are the unit vectors along the x and y directions. In second-order perturbation theory the diamagnetic shift is then estimated to be

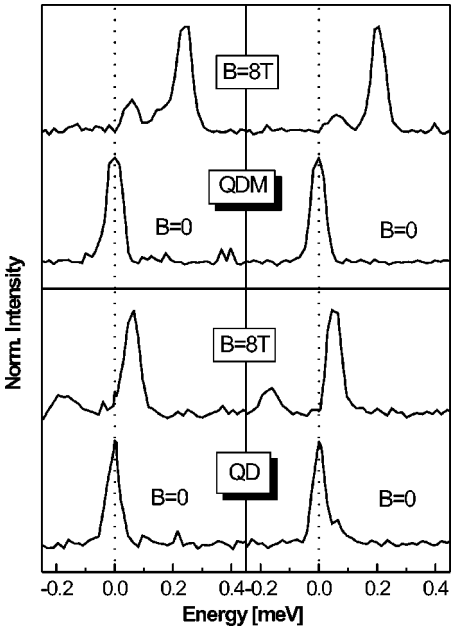

FIG. 23. Upper panels: Photoluminescence spectra of two InAs/GaAs quantum dot molecules with 8-nm-wide barriers at $B=0$ and 8 T aligned in the Voigt configuration. Lower panels: The corresponding spectra of two quantum dots from the single layer reference sample. To facilitate comparison, the zero-field transition energies have been set to zero in each case.

$$\Delta E=\frac{e^2}{2}\left(\frac{\langle z_e^2\rangle}{m_e}+\frac{\langle z_h^2\rangle}{m_h}\right)B^2, \tag{6}$$

with the electron and hole masses m_e and m_h along z, respectively. Here $\langle z_j^2\rangle=\langle S_i|z_j^2|S_i\rangle$, $j=e,h$, are the mean extensions of the electron and hole wave functions parallel to the molecule axis for state $|S_i\rangle$. To obtain the expression Eq. (6), we have used an adiabatic approximation for the exciton wave function due to the much stronger quantization along z than normal to z. Therefore the carrier motions in the molecule plane and perpendicular to it can be separated and the exciton wave function can be written as $\Psi_X=\psi_X(x_e,y_e;x_h,y_h)\zeta(z_e)\zeta(z_h)$.

The spectra of two 8 nm barrier quantum dot molecules which in Faraday configuration show a doublet splitting are shown in the two upper panels of Fig. 23 for $B=0$ and 8 T, oriented normal to the molecule axis. For comparison also corresponding spectra of two single quantum dots from the reference sample are shown in the two lower panels. For the designated molecules the shift is roughly three times larger than that in the quantum dots. While for the dots the shift is about 0.07 meV up to 8 T, for the molecules the shift is more than 0.2 meV. Thus the wave function is clearly much more extended for QDM1 and QDM2, suggesting that these two structures can indeed be identified as electronically coupled quantum dots. To be clear we note that from the data it cannot be concluded whether (in a single particle picture) both electron and hole wave functions form extended states, or whether the increased shift is due to the electron only.

For completeness we give here also the diamagnetic shift data that are observed for a molecule of reduced symmetry

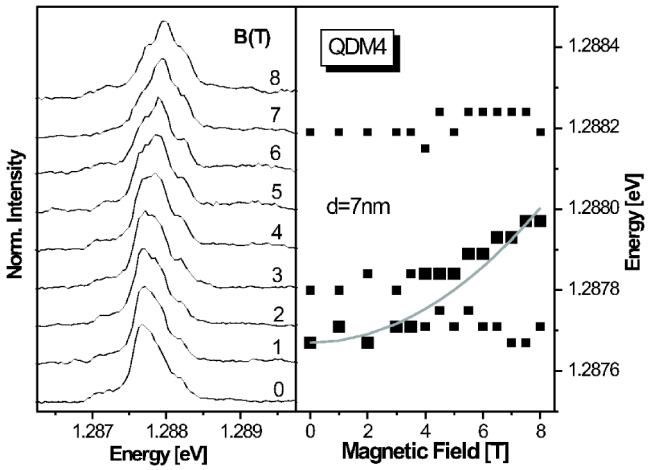

FIG. 24. Left panel: Photoluminescence spectra of the QDM4 in Ref. 19 at different magnetic fields in the Voigt configuration. Right panel: The resulting magnetic field dispersion of the transition energies. The symbol sizes give the relative emission line intensities. The gray line indicates the diamagnetic shift assuming a form proportional to B^2.

(QDM4) under the experimental condition of the Voigt configuration. The photoluminescence spectra of QDM4 at different magnetic fields are shown in the left panel of Fig. 24. At zero field a broad emission band consisting of a few emission lines is observed, but it is hard to determine the number of contributing transitions. Resolved can be an intense low-energy feature and a feature of weaker intensity shifted by $\sim$0.1 meV to higher energies. Also another feature, roughly 0.4 meV above the lowest-lying line, is observed. Their energies, whose magnetic field dispersion is shown in the right panel of Fig. 24, have been determined by a line-shape analysis. Among the two low-energy lines apparently an anticrossing occurs, as seen from the exchange of intensity (oscillator strength) between them. While up to 3 T the low-energy feature is the stronger one, at higher fields the high-energy feature becomes dominating, as indicated by the size of the symbols which give the relative emission intensities. The diamagnetic shift in this case is taken as the shift of the high-intensity line, which follows in good approximation a B^2 dependence, as indicated by the gray line in Fig. 24. This shift of more than 0.25 meV up to $B=8$ T is considerably larger than the shift in quantum dots, giving further support for the molecule character, for the asymmetric structures also.

This shift may be contrasted with the shift that is observed in the Faraday configuration (see Sec. V D), which tests the extension of the wave function in the molecule plane. In the Faraday configuration the shift is determined by the in-plane size of the dot structures that form the molecule which is large as compared to their height ($\sim$20 and $\sim$2 nm, respectively). We find a shift of the center of the fine structure multiplet by 0.4 meV up to $B=8$ T, less than twice as large as the shift in the Voigt configuration. This comparison underlines the extended character of the molecule wave function across the barrier, and can be analyzed more quantitatively: in Faraday configuration ($\mathbf{B}=B\mathbf{e}_z$) the vector potential can be chosen as $\mathbf{A}=Bx\mathbf{e}_y$, resulting in a diamagnetic shift:

$$\Delta E = \frac{e^2}{2}\left(\frac{\langle x_e^2\rangle}{m_e}+\frac{\langle x_h^2\rangle}{m_h}\right)B^2. \tag{7}$$

Assuming that the diamagnetic shift is dominated by the electron with a small isotropic mass, the ratio of the shifts in Faraday and Voigt configurations is given by

$$\frac{\Delta E[\mathbf{B}\|\mathbf{e}_z]}{\Delta E[\mathbf{B}\|\mathbf{e}_x]} \approx \frac{\langle x_e^2\rangle}{\langle z_e^2\rangle}. \tag{8}$$

From the experiments this ratio was estimated to be about 2 (see also Sec. IV). Using the in-plane molecule radius of 10 nm as estimate of the in-plane extension $\langle x_e^2\rangle^{1/2}$ of the electron wave function (certainly slightly overestimating the mean wave function extension), we obtain for the vertical extension $\langle z_e^2\rangle^{1/2}\approx 7$ nm. This value is in good accord with the effective molecule thickness from dot center to dot center. This separation can be estimated from the microscopy data by two times one-half the dot height plus the effective barrier width, which is 2×1 nm$+(5-6)$nm$=8$ nm (see Sec. II), which is in reasonable accord with the simple estimate given above.

For consistency we cross-check the 7 nm value also with the value for the quantum dot. In Voigt configuration the ratio of molecule and dot shifts is given by

$$\frac{\Delta E_{\mathrm{QDM}}[\mathbf{B}\|\mathbf{e}_x]}{\Delta E_{QD}[\mathbf{B}\|\mathbf{e}_x]} \approx \frac{\langle z_e^2\rangle_{\mathrm{QDM}}}{\langle z_e^2\rangle_{QD}}, \tag{9}$$

assuming again the same electron masses in the two structure types. From the averaged values in Fig. 25 we obtain here a ratio of about 3.5. Taking the value of 7 nm for the molecule, we obtain for the quantum dot a value of slightly less than 4 nm, which overestimates the value of 2 ± 1 nm, but still is acceptable on the base of our simple estimate.

The diamagnetic shift in Voigt configuration is shown in Fig. 25 as a function of magnetic field for various 8 nm barrier quantum dot molecules. The data shown by the symbols are the values obtained by averaging the shifts for different molecule structures. The bars do not correspond to the error of the measurement ($\sim$20 μeV in this case) but give the variation of the data for the different structures. In all studied cases the shift is at least 0.2 meV at $B=8$ T; in some cases it exceeds 0.25 meV. The dotted line indicates the shift in the quantum dots which remains clearly below 0.1 meV. This demonstrates that for all the studied quantum dot molecules with $d=8$ nm the wave function is much more extended than in the dot case, even though the field dispersions might look very different due to structural variations, as seen from the comparison of the data in Figs. 18 and 22.

Coming back to the fine structure splitting of QDM1- and QDM2-like structures in the Faraday configuration, Fig. 26 shows the polarization-resolved emission of another quantum dot molecule with a barrier width of 8 nm up to 7 T for this field orientation. A splitting into a doublet is seen, similar to the observations for QDM1. While the emission from QDM1 is fully circularly polarized in magnetic field, the behavior is more complicated for the molecule structure of Fig. 26: the high-energy line evolves as purely σ^- polarized, but the low-energy line is a superposition of both circular

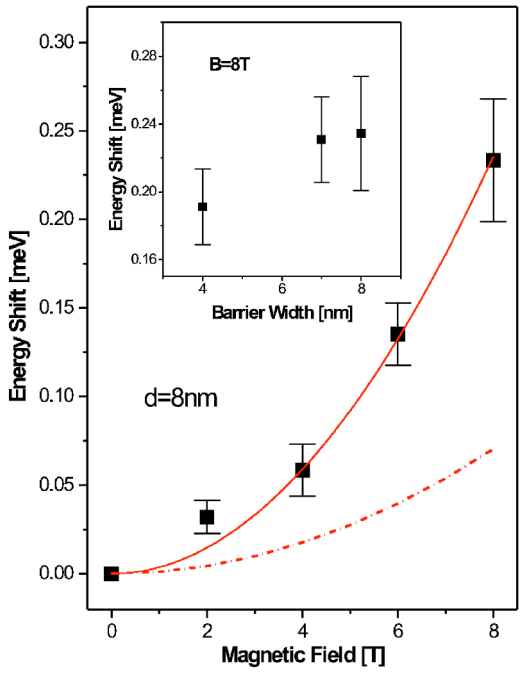

FIG. 25. Diamagnetic shift of the exciton emission in InAs/GaAs quantum dot molecules with an 8-nm-wide barrier as a function of magnetic field in the Voigt configuration (the symbols). These data have been obtained by averaging the shifts of five different molecules. The bars give the variation of the data for the different structures. The solid line is a fit to the data using a B^2 dependence. The dash-dotted line indicates the corresponding shift for single dots. The inset shows the diamagnetic shift up to 8 T in the Voigt configuration versus the width of the molecule barrier.

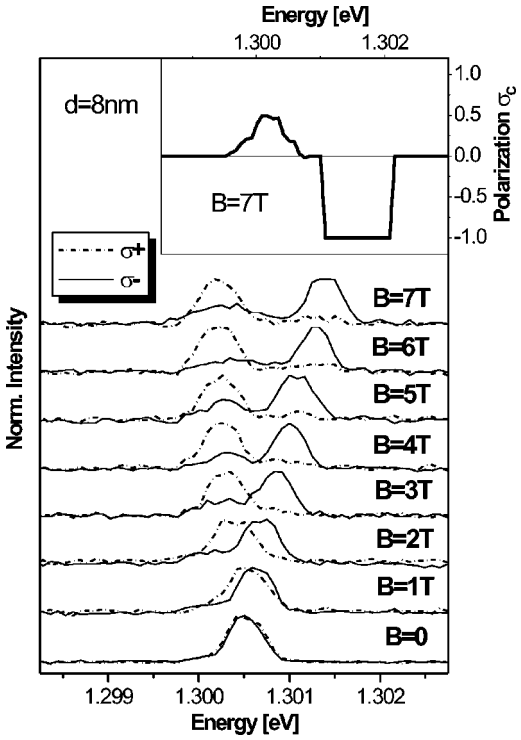

FIG. 26. Circular-polarization-resolved photoluminescence spectra of an InAs/GaAs quantum dot molecule with an 8-nm-wide barrier for different magnetic fields (Faraday configuration). The inset shows the circular polarization degree σ_C that has been determined from the $B=7$ T spectra as a function of emission energy.

polarizations up to the highest B. The outcome of this is the spectral dependence of the circular polarization σ_C that is shown for $B=7$ T in the inset of Fig. 26. On the low-energy side of the emission a maximum polarization below 50% is obtained, but it changes over to 100% on the high-energy side.

Finally let us discuss QDM5, for which we observed two closely spaced emission lines at zero field, in contrast to the other four molecule structures of Ref. 19. Photoluminescence spectra of QDM5 are shown in the left panel of Fig. 27, the corresponding magnetic field dependence of the transition energies is summarized in the right panel. To obtain it, the circular polarization of the emission was also analyzed (see below). Each line shows predominantly a doublet splitting in magnetic field. The field strengths available in the experiment were too small to bring the two fine structure doublets into resonance and to search for anticrossings. In addition to the strong spectral features, some weak contributions of dark exciton emission are found. At first look, it seems that in this case we address two independent quantum dots that do not show any coupling. However, taking a closer look, there are two observations that set the QDM5 data apart from the observations that would be made for decoupled dot structures.

For an exciton in a strongly confined quantum dot, the diamagnetic shift is positive definite, as demonstrated by numerous single dot studies and by theoretical calculations.[36,37] Figure 28 shows the diamagnetic shifts of the two zero-field emission lines, which have been obtained by averaging the energies of the magnetic-field-split components in each case. Surprisingly, at low fields a negative diamagnetic shift is observed. This shift is rather weak for the lower-lying line (up to 0.05 meV for $B\sim 2$ T), and it is more pronounced for the higher-lying line (more than 0.1 meV). For higher fields both shifts are reversed toward positive energies.

Negative diamagnetic shifts are known, for example, for charged excitons in higher-dimensional systems.[38] They result from a spatial redistribution of the carrier wave functions that form the excitonic complex, leading to an enhancement of the Coulomb interaction that lowers the complexes' energy more strongly than its increase due to the magnetic confinement. In single quantum dots such a redistribution is not possible.[39] This observation therefore indicates that QDM5 cannot be treated simply as two independent, decoupled quantum dots. Translating the concept that a negative diamagnetic shift results from a carrier redistribution also to the case of quantum dot molecules, the present data might indicate that localization of a carrier in one of the quantum dots is lifted by applying a magnetic field. This could occur, e.g., by bringing two hole levels into resonance.

The coupling of the dots in QDM5 is also supported by the magnetic field dependence of the spin splitting of the emission lines, as shown in Fig. 29. Below 5 T the low-energy line shows a rather small splitting, while the splitting of the high-energy line is considerably larger. Both splittings depend linearly on magnetic field in this field range. However, when entering the high-field regime above 5 T this

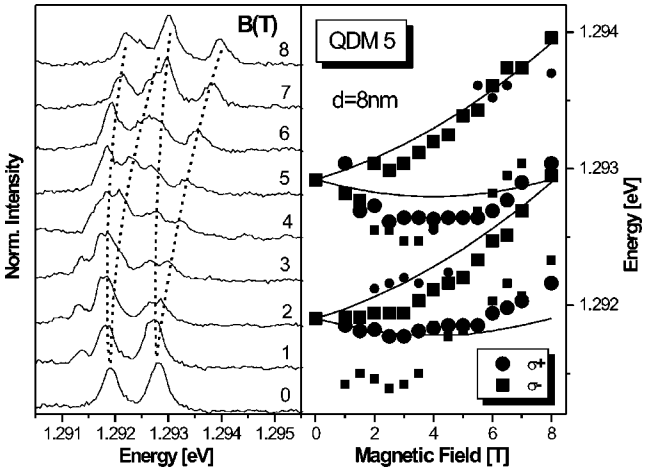

FIG. 27. The left panel shows photoluminescence spectra of QDM5 in Ref. 19, recorded at different magnetic fields in the Faraday configuration. Lines guide the eye. The right panel gives the resulting magnetic field dispersion of the transition energies. The symbols give the experimental data. The symbol shapes indicate the dominant circular polarization; their sizes give the relative emission intensities. For the lines we assumed identical diamagnetic shifts and spin splittings, as would be approximately the case for two decoupled, independent quantum dots.

behavior changes, as indicated by the solid and dash-dotted lines which serve as guides to the eye. The splitting of the lower-lying line changes over into a much stronger field dependence, while that of the higher-lying line saturates. This is a behavior that as well distinguishes QDM5 from isolated quantum dots.

For (nonmagnetic) self-assembled dot structures, to the best of our knowledge, only spin splittings depending linearly on B have been observed (neglecting minor effects of electron-hole exchange interaction, which are important at small fields only).[40] This also indicates, that heavy hole–light hole mixing is small for these dot systems. In general, the hole mixing is changed by a magnetic field, potentially resulting in strongly nonlinear dependencies of the splittings versus B, as observed for quantum wells, for example.[41] The data for QDM1 and QDM2 with their linear splittings (see inset of Fig. 29) suggest that also for coupled quantum dots the heavy hole–light hole mixing is small, at least for the ground state exciton. Alternately the nonlinearities for QDM5 might originate from redistributions of the carrier wave functions. Such a redistribution over the molecule structure could change the g factors of electron and hole, which add up to the exciton g factor: they are obtained by averaging the corresponding contributions from each of the heterostructure constituents with the respective wave function weights. As a further alternative, the abrupt changes of spin splitting could also point to the emergence of an anticrossing at high fields, in conjunction with the related exchange of state character, since the two middle energy levels approach each other for $B>6$ T.

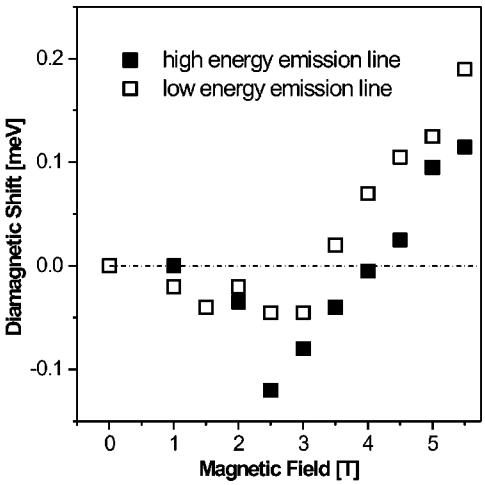

FIG. 28. Diamagnetic shifts of the two emission line centers that originate from the $B=0$ features for QDM5 of Ref. 19 versus magnetic field in the Faraday configuration.

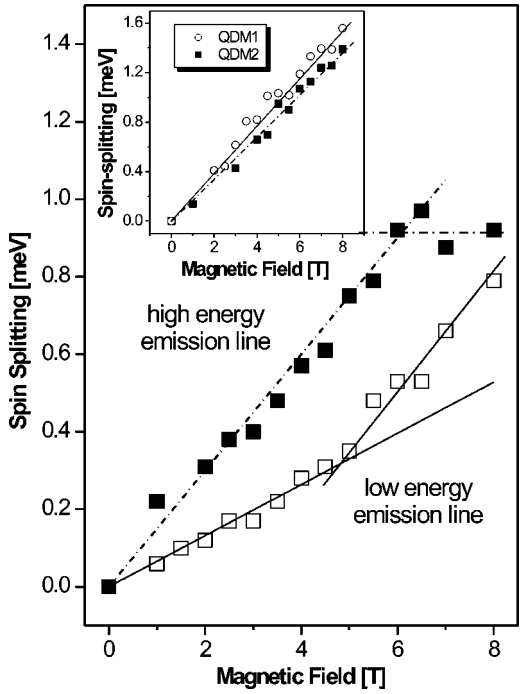

FIG. 29. Zeeman splitting of the two spectral lines that are observed at $B=0$ for QDM5 of Ref. 19, as a function of the magnetic field (Faraday configuration). The solid and dash-dotted lines are guides to the eye. For comparison, the inset shows the magnetic field dependence of the exciton spin splitting for QDM1 and QDM2.

As these findings strongly hint at a coupling of the two dots also for QDM5, we can try to relate the features observed for it to the states developed in the exciton model above: the experimental situation for this molecule structure is similar to the one that we found in the calculation of energies and wave functions for strongly asymmetric molecule structures. The low-energy line at $B=0$ would be attributed then to emission from state $|S_1\rangle$, while the high-energy line would arise from $|S_2\rangle$ state recombination. These states are mixed through an asymmetry in the molecule structure and share oscillator strength. The symmetry breaking is so strong that the oscillator strength is almost equally distributed among the two features.

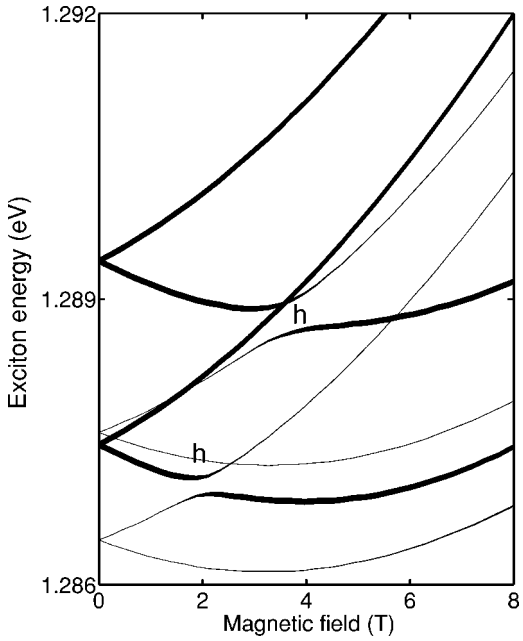

FIG. 30. Calculated exciton fine structure splitting in magnetic field for an asymmetric molecule with an 8-nm-wide barrier (see text for structural details). The energy range of states $|S_1\rangle$ and $|S_2\rangle$ is shown. The labels "h" indicate anticrossings which arise from level repulsion among hole levels.

The exciton fine structure pattern shows a very strong resemblance to that modeled for a molecule with strong asymmetry in Ref. 30. For these calculations the dot confinement potentials were taken to differ by 3% for electron and hole and the dots are laterally displaced by 4 nm. As confinement potential heights we used here 600 and 620 meV for the electrons, as well as 100 and 103 meV for the holes. The rest of the parameters were identical to those given above in Sec. IV. The calculated field dispersion of the fine structure is shown in Fig. 30. At zero field, the fine structure multiplet is dominated by two strong emission lines. In addition to the equal distribution of oscillator strength among them, the energy separation between these lines corresponding to $|S_1\rangle$ and $|S_2\rangle$ is close to the experimentally observed value for QDM5. Due to the anticrossings the field-induced splitting of each doublet depends highly nonlinearly on B, in qualitative agreement with experiments.

As an intermediate summary of the very diverse behaviors that are observed for the exciton fine structure splitting in the wide barrier samples, one more time the polarization of the quantum dot molecule emission will be considered. The three left-hand panels of Fig. 31 show circularly polarized emission spectra of QDM1, QDM3, and QDM5 of Ref. 19 at $B=7$ T. These structures cover the whole range of observed structural symmetries, from very high to very low. For QDM1 the two split emission lines are fully circularly polarized, as indicated already above. Six spectral features can be clearly resolved for QDM3. None of these lines, however, shows full circular polarization. This is also true for QDM5, for which four dominant emission lines are seen, all of them with mixed polarizations.

The circular polarization degrees that are obtained from these traces are shown in the three right-hand panels. When

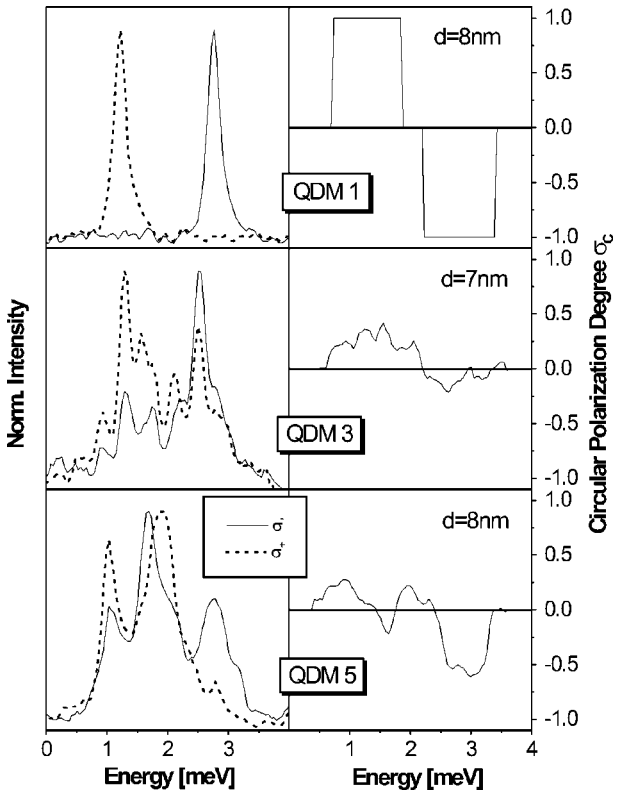

FIG. 31. The left panels give circularly polarized emission spectra of QDM1, QDM3, and QDM5 of Ref. 19 at $B=7$ T. The right panels show the corresponding circular polarization degrees as functions of emission energy. To facilitate comparison, the energy ranges in which the emission occurs have been shifted toward zero energy. 4 meV is shown in each case.

scanning in energy over the emission range of interest, QDM1 shows the same "digital" switching of σ_C as seen for single dots. QDM3 shows a behavior very similar to that observed above for QDM4. The behavior with the widest fluctuations is seen for QDM5, for which the circular polarization oscillates between positive and negative values and is never larger than about 50%.

For qualitative comparison, Fig. 32 gives the calculated circular polarization degrees for two different quantum dot molecules, each with an 8 nm barrier: an ideal one (the left panel) consisting of two identical quantum dots with perfect vertical alignment, and an asymmetric one (the right panel). The structural parameters for the latter case were the same as those for calculating the magnetic field dispersion of the exciton fine structure in Fig. 30.[30] The polarization degrees σ_C are given by the heights of the columns that are positioned at the energies of the different exciton fine structure states. Their relative optical activities are given by the column widths. Note that for the transitions with oscillator strength close to zero the column width has been slightly increased artificially, for better visualization. The relative oscillator strengths are therefore indicated also by the numbers at each column.

As for the calculation of the exciton energies we did not push for a quantitative agreement between experiment and theory in the modeling for which a precise knowledge of all

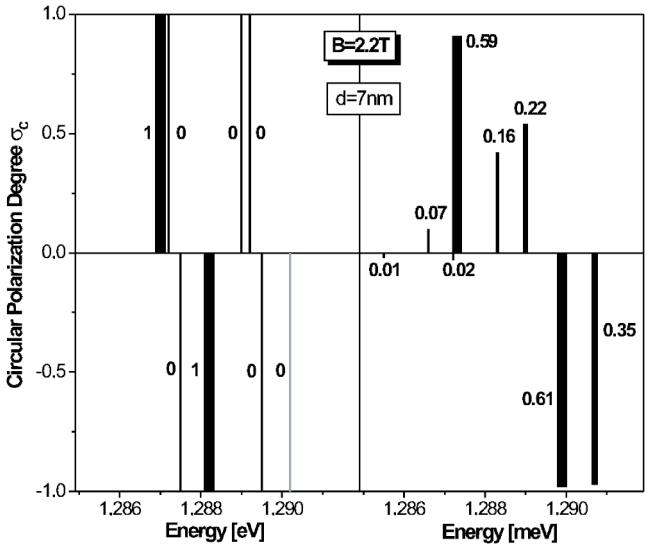

FIG. 32. Calculated circular polarization degrees for a highly symmetric quantum dot molecule consisting of two identical quantum dots that are perfectly vertically aligned (the left panel) and a molecule consisting of two different quantum dots (see text for details) with some lateral displacement (the right panel). Shown are the σ_C for the several spectral lines that belong to the $|S_1\rangle$ and the $|S_2\rangle$ fine structure multiplets. The widths of the columns give the oscillator strengths of the transitions, the values of which are given by the numbers at each column as well.

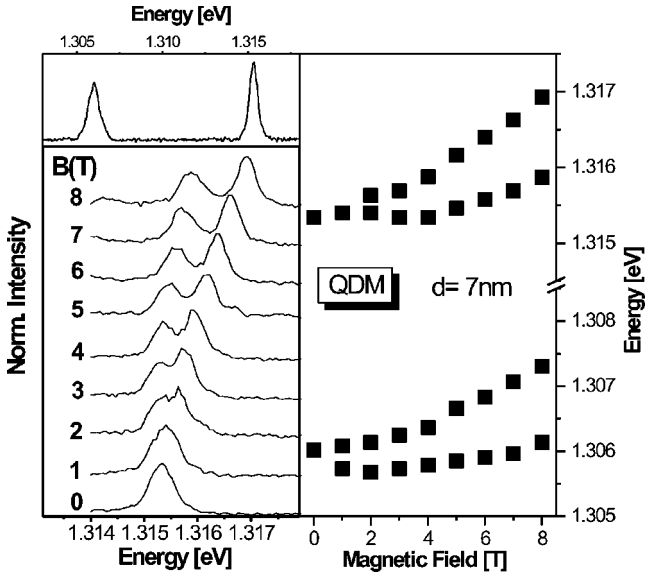

FIG. 33. The upper left panel shows a photoluminescence spectrum of a quantum dot molecule with a 7-nm-wide barrier, which shows a behavior similar to QDM1 of Ref. 19. The full spectral range in which the exciton states $|S_1\rangle$ to $|S_4\rangle$ are expected is shown. The lower left panel zooms into the energy range in which the high-energy line is located and shows spectra at different magnetic fields (Faraday configuration). The right panel gives the field dispersion of the transition energies observed for the zero-field emission lines.

molecule parameters would be required. The main goal instead was to understand the impact of the observed anticrossings, which arise from mixing of different spin configurations, on the circular polarization of the emission. In the experiment, for asymmetric molecule structures such as QDM3 or QDM4, strong state mixings take place even at high magnetic field strengths, for which we have also analyzed σ_C, because the spectral lines are energetically well separated at $B=7$ T and thus can be well distinguished. To have a situation comparable with experiment, we have calculated the circular polarization for the low-symmetry molecule structure also at a field strength at which pronounced anticrossings occur. For the somewhat arbitrary choice of molecule asymmetry parameters this occurred at $B=2.2$ T. For consistency, σ_C was then calculated at this field strength also for the high-symmetry structure. For comparing theory and experiment, the same remarks about the relation of oscillator strength and emission intensity apply as above in the discussion of the anticrossings.

From the results in Fig. 32 one sees that for the ideal molecule structure (the left panel) full circular polarization is observed, as in the experiment for QDM1. This holds for all the states of the fine structure multiplets $|S_1\rangle$ and $|S_2\rangle$. Turning to the asymmetric structure (the right panel), six fine structure states have significant oscillator strength, in contrast to only two lines visible in the high-symmetry case. Basically none of the lines exhibits complete circular polarization, even though three lines come close to full polarization. Generally the calculations show a slightly larger polarization degree than observed experimentally. There might be several reasons for this: for example, in the model we assume a pure heavy hole character for the valence band ground states. If light hole states are ever mixed into these states, this admixture will lead to a considerable reduction of the polarization degree.

B. Fine structure of the "antibonding" exciton states in the wide barrier samples

The previous considerations immediately raise the question of how the structural variations affect the fine structure of the higher-lying, tunnel-split exciton states. The exciton states $|S_3\rangle$ and $|S_4\rangle$ contribute to their patterns. Some data for them will be presented in the following. Similar to $|S_1\rangle$ and $|S_2\rangle$, the energy levels $|S_3\rangle$ and $|S_4\rangle$ are located quite close to each other ($\sim$1 meV separation) in 7- and 8-nm-wide barrier samples for not too strong asymmetry (see Fig. 9), so that a magnetic field can induce resonances among them. Each state offers four different spin configurations, so that the high-energy fine structure multiplet is formed by eight states in total, as in the case of the "bonding" state energy range. In molecules of "perfect" symmetry only state $|S_4\rangle$ would be observable. In magnetic field this state would show a doublet splitting, as only the two excitons with momentum $|M|=1$ can couple to the light field.

Figure 33 gives an example of a molecule with a behavior that seems very close to the ideally expected one. The upper left panel shows the zero-magnetic-field emission spectrum over the total energy range, in which the four exciton states $|S_i\rangle$ are located. The emission consists of two lines, which we attribute to emission from states $|S_1\rangle$ and $|S_4\rangle$ that are sepa-

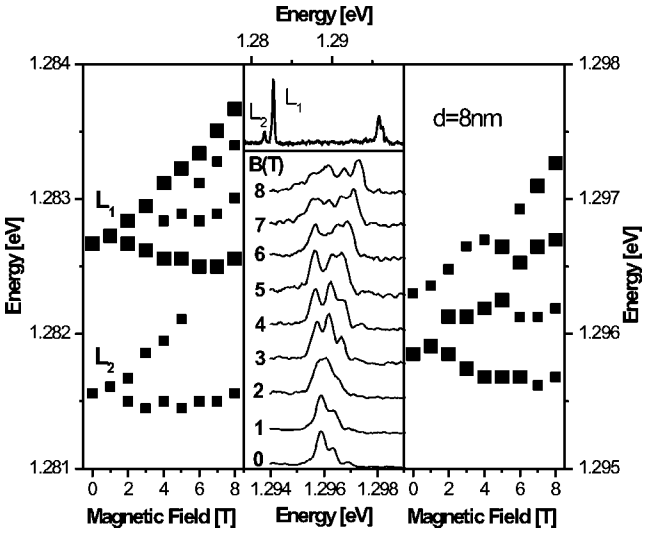

FIG. 34. The upper middle panel shows a $B=0$ emission spectrum of a quantum dot molecule with an 8-nm-wide barrier. The full spectral range in which the exciton states $|S_1\rangle$ to $|S_4\rangle$ are expected is shown. The left panel gives the magnetic field dispersion of the state multiplet that emerges from the low-energy emission features. The lower middle panel shows spectra for the energy range in which states $|S_3\rangle$ and $|S_4\rangle$ are located at different magnetic fields (Faraday configuration). The right panel gives the resulting field dependence of the transition energies in this range. The symbol sizes in the left and right panels indicate the relative intensities of the transitions.

rated by 9 meV. $|S_2\rangle$ and $|S_3\rangle$ apparently do not contribute to the emission. The right panel gives the magnetic field dependence of the doublet of lines, which arises from the splitting of the low-energy $|S_1\rangle$ emission. Its behavior is very similar to that of QDM1. The lower part of the left panel shows the magnetic-field-induced splitting of the high-energy emission line $|S_4\rangle$. For it also a doublet splitting is observed, in agreement with our expectations. The splitting is linear in magnetic field, and its magnitude is very comparable to that of $|S_1\rangle$ (1.2 meV at 8 T). However, it has a considerably larger diamagnetic shift of about 0.9 meV up to 8 T, as compared to 0.4 meV for $|S_1\rangle$.

Figure 34 shows another example of a quantum dot molecule with an 8-nm-wide barrier which seems to have a slightly enhanced asymmetry as compared to the structure just discussed. In the low-energy range two emission lines are observed, a dominant one labeled L_1 and one with rather weak intensity labeled L_2, which is shifted by 1.2 meV to lower energies. In magnetic field L_2 becomes even weaker so that it can hardly be resolved. The fine structure splitting of these two lines is shown in the left panel. L_1 shows mostly a doublet splitting with two weak emission features appearing in between. This molecule structure is thus similar to QDM2. The splitting of the lower-lying feature L_2 follows closely that of the outer doublet from L_1. The origin of L_2 is not fully clarified, but it most probably does not belong to the fine structure multiplet of the charge neutral exciton. Tentatively we assign it to emission from negatively charged exciton complexes for which we would expect a similar splitting pattern as for the neutral ones, except for vanishing fine structure splittings.[31]

The lower middle panel zooms into the energy range of states $|S_3\rangle$ and $|S_4\rangle$ showing photoluminescence spectra at different magnetic fields. At zero field the emission consists of two lines, one with dominant intensity at lower energies, and one of weaker intensity on the high-energy side. There is another weak line shifted even more to higher energies, but this one fades quickly away in magnetic field and is not of further interest here. When ramping B, the emission lines split. Their linewidths are slightly increased as compared to the widths observed for the lines of the "bonding" exciton state. This linewidth increase might indicate that the exciton lifetime is reduced due to the additional decay channel that is offered by relaxation into the molecule ground states. Still they are quite sharp as expected for the case of reduced relaxation. Among the features apparently redistributions of oscillator strength take place, hinting at avoided crossings also for the higher-lying exciton states. Plotting the transition energies as functions of magnetic field (see the right panel of Fig. 34) confirms the underlying level repulsions. Their origin has to be attributed again to a quantum dot molecule asymmetry, as in case of the low-energy fine structure multiplet. Also here the diamagnetic shift of the higher-lying feature is considerably enhanced as compared to that of the low-energy line.

Finally let us turn to the QDM4 structure that has been discussed already before. The complicated behavior of the exciton fine structure occurring within the $|S_1\rangle$ and $|S_2\rangle$ state multiplet pointed at a considerable symmetry breaking for this molecule. This is reflected also by the fine structure of the higher-lying exciton states. In their energy range a splitting into two spectral features of equal intensities is observed at zero field (see the upper left panel of Fig. 35). How these lines behave in magnetic field is shown in the lower left panel. Again the linewidths are increased as compared to those on the low-energy side, hindering the resolution of their magnetic field dispersions. Irrespective of this restriction, also here strong variations of the emission intensities are observed, which point toward an exchange of oscillator strength among fine structure states and thus at anticrossings. These processes are, however, hard to distinguish (see the right panel) as multiple state mixings seem to occur.

To sum up the results of Secs. V A and V B, within the developed statistics the fine structure of the exciton states gives a consistent picture of molecule coupling. Whenever for the low-lying "bonding" state a doublet splitting is observed, indicating a rather high molecule symmetry, for the high-lying "antibonding" state a doublet splitting also appears. When, on the other hand, the low-lying states show a more complicated splitting pattern due to symmetry reduction; this is reflected also by the splitting of the higher-lying levels.

For the molecule structures with a structural asymmetry anticrossings are observed in magnetic field dispersions up to the highest fields of 8 T (see Figs. 18 and 20). One might argue that even more emission lines appear in the spectra and become involved in avoided crossings when ramping the magnetic field above 8 T. If the total number of emission lines exceeds eight then this would prevent our attribution of the emission lines to the fine structure multiplets of states $|S_1\rangle$ and $|S_2\rangle$. To exclude this we have recently performed single molecule experiments up to 28 T.[42]

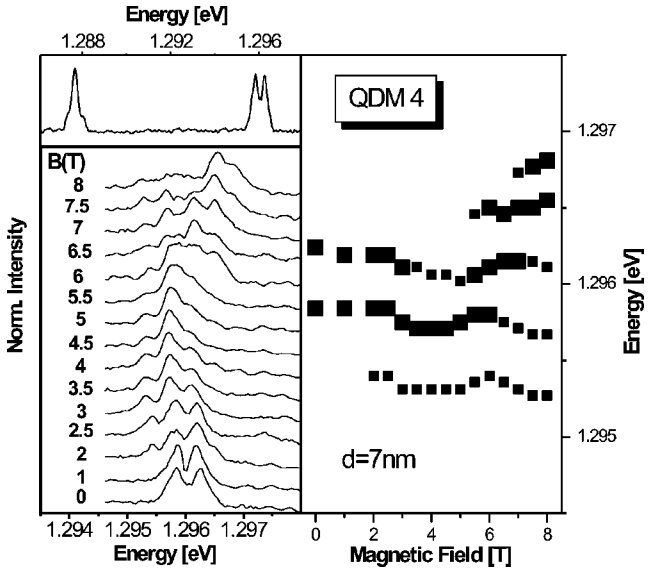

FIG. 35. Same as Fig. 33, but for QDM4 of Ref. 19. The fine structure splitting pattern of the ground state exciton was shown already in Fig. 18. The emission within the energy range of all states $|S_i\rangle$, $i=1,\ldots,4$, is given in the upper left panel at $B=0$. The lower left panel zooms into the high-energy range of the $|S_3\rangle$ and $|S_4\rangle$ states at different magnetic fields. The right panel gives the corresponding field dependence of the emission lines observed there. Symbol sizes indicate relative intensities.

Figure 36 shows a contour plot composed of photoluminescence spectra recorded from $B=0$ up to 28 T in steps of 1 T. The spectra were recorded on a molecule with an 8-nm-wide barrier. The zero-field emission is dominated by two lines, a dominant one at about 1.283 eV and a weaker one at ~1.296 eV, which correspond to the "bonding" and "antibonding" exciton states. There is also a weaker feature ~1 meV below the bonding state which we attribute to trion

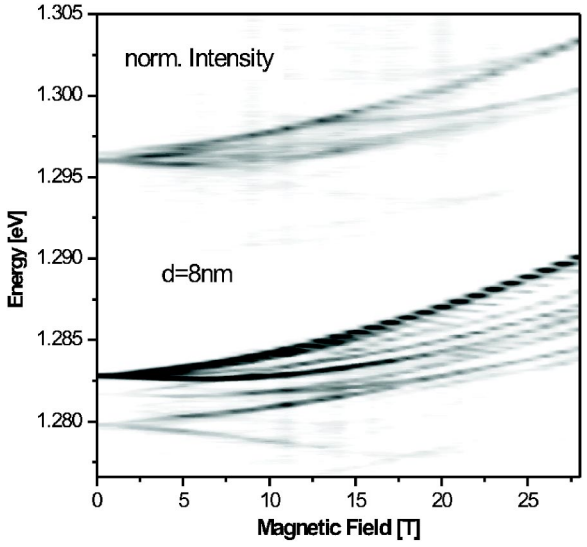

FIG. 36. Contour plot of photoluminescence spectra recorded on an 8 nm barrier InAs/GaAs molecule structure of rather low symmetry in magnetic fields up to 28 T. The plot is composed of spectra recorded in steps of 1 T at $T=4.2$ K.

emission (see before). It shows a simple doublet splitting in magnetic field as can be expected since it represents a hole interacting with a spin singlet electron pair state so that spin-related splittings vanish at zero field. Therefore it is not of further interest here and will not be considered anymore. For these studies the excitation power had to be increased to obtain enough signal. At these excitation levels also indications for biexciton emission are found in the spectrum slightly below 1.280 eV. In magnetic field it shows a dominant doublet splitting, but its intensity is too weak to make any conclusive statements about its fine structure. It will also not be discussed in further detail here.

For both the bonding and antibonding states some complicated anticrossings appear as the magnetic field is ramped, with details again different from previous structures. However, in both cases the number of observed features is equal to or less than eight, so that we can also set a clear upper limit of 16 for the total number of spectral features for the *s*-shell molecule excitons. This gives a powerful confirmation of the discussion in the two preceding sections.

For comparison, equivalent studies have been also performed on a molecule structure of high symmetry, as shown in Fig. 37. Here we observe predominantly doublet splittings for both the "bonding" as well as the "antibonding" exciton states. Interestingly, we find here in the high-field regime deviations from a linear dependence of the spin splitting on magnetic field, as shown for the "bonding" exciton in the lower panel of Fig. 37 and indicated by the lines. The origin of this nonlinearity could be heavy hole–light hole mixing induced by these very high field strengths. Within the experimental accuracy the splitting of the "antibonding" state is basically identical to that of the "bonding" one.

At the end of this section we comment on the circular polarization of the high-energy exciton states in the molecules. In the experiment we find for them behaviors which are very similar to those for the low-energy states (in the low-field regime). A wide spectrum ranging from complete to fully mixed polarization is observed. Through the calculations this diversity again can be traced to variations of the molecule symmetry.

C. "Bonding" exciton fine structure pattern in narrow barrier samples

After discussing and detailing further the data presented in Ref. 19 for the molecule structures with barrier widths of 7 and 8 nm, we turn now to the presentation of the exciton fine structure for quantum dot molecules with narrower barriers, for which the tunneling splitting is very much enlarged. Let us discuss first what can be expected for the fine structure within the frame of our simple exciton model by recalling the starting situation for the wide barrier samples. In their case the energy splitting between the exciton states $|S_1\rangle$ and $|S_2\rangle$ is so small (see Fig. 9) that a magnetic field can bring them into resonance. A reduced structural symmetry induces a significant mixing within the $|S_1\rangle$ and $|S_2\rangle$ multipletts, resulting in the described anticrossings. In structures of rather high symmetry this mixing is, however, too weak to make state $|S_2\rangle$ visible, as demonstrated above.

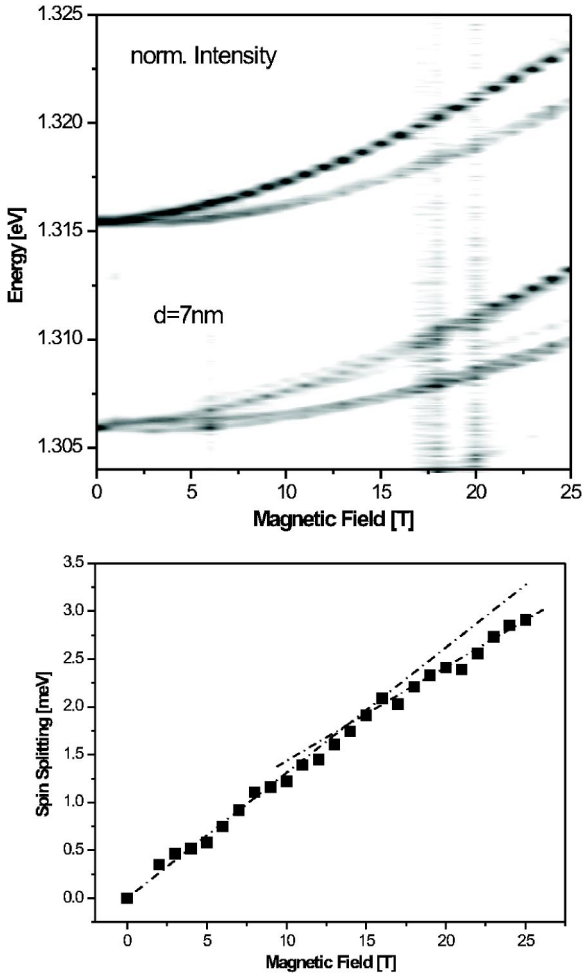

FIG. 37. Upper panel: Contour plot of photoluminescence spectra recorded on a 7 nm barrier molecule structure of rather high symmetry in magnetic fields up to 25 T in steps of 1 T. Lower panel: Spin splitting of the "bonding" exciton state as a function of magnetic field. The lines guide the eye.

When the barrier width is reduced the splitting between $|S_1\rangle$ and $|S_2\rangle$ increases strongly to reach a magnitude (see Figure 9), that the magnetic field cannot bring them in resonance and induce a significant mixing for the available field strengths.[43] Thus we expect that only $|S_1\rangle$ is involved in the ground state emission of the quantum dot molecules. Figure 38 shows polarization-resolved photoluminescence spectra at different magnetic fields for two quantum dot molecules, one with a 4-nm-wide barrier (the left panel) and one with a 5-nm-barrier (the right panel). In each case the emission is dominated by a doublet of lines. For some narrow barrier molecule structures also indications for dark exciton emission are observed (not shown). However, the maximum number of emission lines is limited to four in all cases, equivalent to the number of possible electron-hole spin configurations.

Note that also for these barrier widths complete circular polarization of the emission is not the rule. The energy dependence of the circular polarization degree σ_C at $B=7$ T is shown in Fig. 39 for the two quantum dot molecules whose spectra have been given in Fig. 38. The polarization for the 4 nm barrier molecule in the top panel shows complete circular

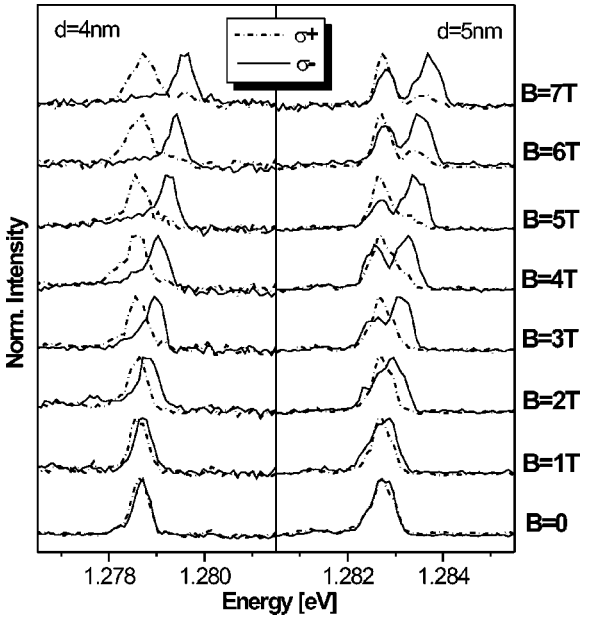

FIG. 38. Photoluminescence spectra of two InAs/GaAs quantum dot molecules with barrier widths of 4 nm (the left panel) and 5 nm (the right panel) recorded at different magnetic fields that were aligned in the Faraday configuration. The circular polarization of the emission has been analyzed.

polarization at this field strength, resulting in a similar "digital" behavior as observed for quantum dots. On the other hand, for the 5 nm barrier molecule no complete polarization is observed (see the bottom panel). While for the low-energy line a strong mixing of right- and left-hand polarizations results in a maximum polarization degree of not more than 20%, the high-energy line is mostly σ^- polarized ($\sigma_C > 50\%$). Thus also for some of these narrow barrier structures a high magnetic field cannot restore the circular polarization.

As mentioned, such a behavior might be explained by light hole admixtures to the lowest confined valence band states. Observations of nonlinearities in the exciton spin splitting would clearly point to such a mixing. However, experimentally we find that the splitting for the narrow barrier samples depends linearly on magnetic field up to 8 T. High-field studies have not been performed yet on these systems. Thus from the present studies it cannot be clearly assessed whether light hole states are important for the lowest-lying excitons. The observation of a doublet or a quadruplet splitting at most also means that it cannot be conclusively decided from the fine structure data whether these systems represent molecules, i.e., whether the two quantum dots are indeed coherently coupled, although it seems reasonable to assume this, since coupling—as demonstrated for the wide barrier case—should be established more easily the narrower the barrier is. This is supported by the observation in transmission electron microscopy that for narrow barrier samples quantum dots with very similar geometries are very well aligned vertically (see Fig. 1). No lateral displacement of the dot structures relative to each other has been resolved for them within the statistics.

In the following two subsections a comparative overview of the exciton diamagnetic shift as well as the exciton spin

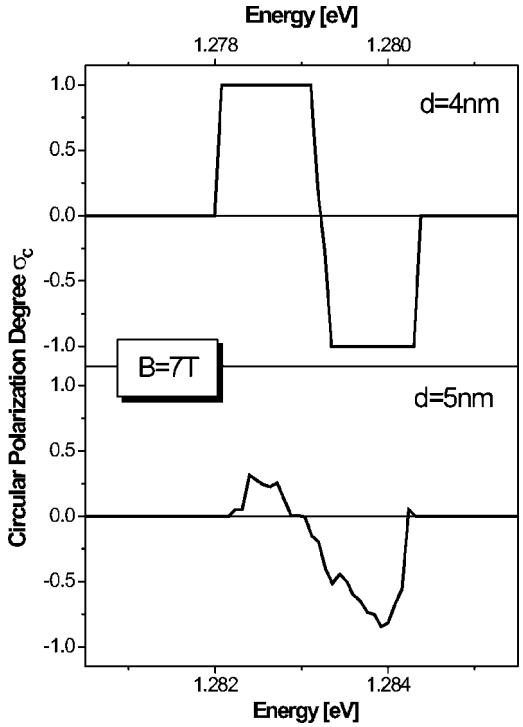

FIG. 39. Circular polarization degree at $B=7$ T as function of emission energy for the quantum dot molecules with 4 nm barrier (the top panel) and 5 nm barrier (the bottom panel) whose spectra have been presented in Fig. 38.

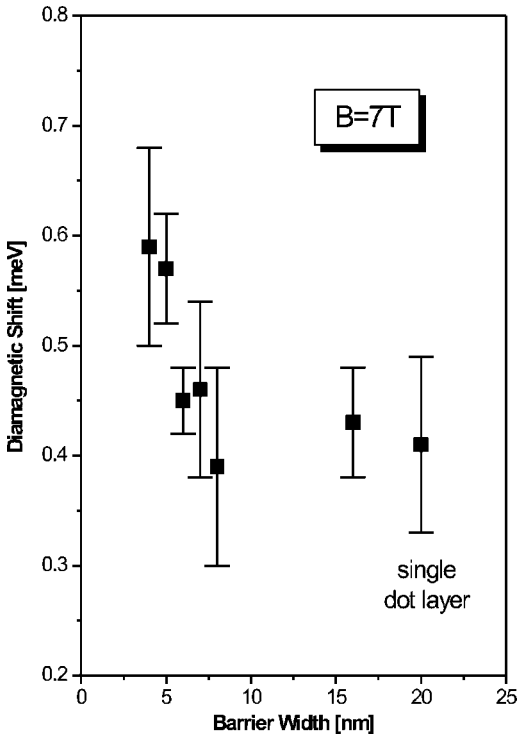

FIG. 40. Diamagnetic shift of the exciton emission up to $B=7$ T (Faraday configuration) as a function of the nominal width of the barrier between the two coupled quantum dots. Each symbol has been obtained by averaging the data of about ten different molecule structures. The bars give the variations of the shifts for different structures with a given barrier width.

splitting is given for the different barrier width samples. For this overview we will restrict attention to structures which essentially show a doublet splitting in magnetic field, in conjunction with a positive diamagnetic shift.

D. Exciton diamagnetic shift

Figure 40 gives the barrier width dependence of the exciton diamagnetic shift in the quantum dot molecules up to 7 T in the Faraday configuration. Shown are the values that have been determined by averaging the data measured for several molecule structures. Note again that the bars do not indicate the error of the measurement (which is ± 50 μeV in this case) but indicate the variation of the shifts for different structures with given barrier width. Also note that data are shown only from structures with a positive diamagnetic shift over the entire magnetic field range. For the single quantum dot sample we observe a shift of ~ 0.4 meV up to 7 T. For the 16 nm barrier sample we find a slightly larger shift. For the molecule samples we find a systematic increase of the shift with decreasing barrier width. For the 8 nm barrier we observe a shift of 0.4 meV, as determined from about ten different molecule structures. For thinner barriers the average diamagnetic shift increases, being slightly less than 0.45 meV for the 6 and 7 nm barrier samples and almost 0.6 meV for the 4 and 5 nm barrier samples.

While we cannot give a quantitative explanation for these observations yet, at least a qualitative discussion is possible, for which we assume a perfectly symmetric molecule structure. The diamagnetic shift is a measure of the extension of the exciton wave function in the molecule plane.[44] For strongly confined quantum dot geometries this extent is closely related to the lateral dot size. This size is supposed to be about the same for the dot structures in the molecules as for the single dot layer reference. However, the shift is also determined by the vertical size of the quantum structure:[44] Coulomb interactions—simply speaking—favor a spherical symmetry of wave functions. This shape becomes distorted by geometric confinement. The Coulomb forces react on this "perturbation" by squeezing the wave function perpendicular to the direction of distortion, trying to restore the spherical shape as much as possible. In quantum wells, for example, the diamagnetic shift decreases with decreasing well width. Let us first discuss the consequences for two quantum dots with height h and height $2h$, which is a situation that is somewhat similar to that of a quantum dot and a quantum dot molecule with very narrow barrier. Due to the smaller height h of the first dot, the exciton wave function is more strongly squeezed in the vertical direction as compared to the second dot with double height $2h$. Therefore the Coulomb interaction enforces a reduction of its lateral extent that is stronger for the first dot than for the second one, which will be directly reflected by their diamagnetic shifts.

This consideration explains the relation of the diamagnetic shifts for quantum dots and narrow barrier quantum dot molecules, but it does not offer an explanation for the systematic barrier width dependence. To understand this behavior, the exciton wave function in the molecules needs to be

considered in more detail. For wide barriers the wave function is concentrated in the two dots of the molecule, whereas the penetration into the barrier is small (see Fig. 10). In each dot the shape of the wave function is similar to that in a single dot, except for its normalization. Thus the diamagnetic shift to a good approximation will be given by the sum of the contributions from each of the two dots. Assuming a symmetric molecule structure consisting of identical dots, the diamagnetic shifts in the dots will be the same and will add up to a value similar to the shift in a single dot. When the barrier becomes narrower, the penetration of the carriers into the barrier increases so that simply speaking the wave functions in the two dots become spatially connected. This leads to an effective increase of the spatial coherence volume along the molecule axis, enabling a larger in-plane exciton extension (a larger diamagnetic shift). Finally the narrow barrier situation described above is reached. This model may explain the rather smooth increase of the diamagnetic shift when going from wide barrier to narrow barrier molecules.

An asymmetry of the molecule structure affects the vertical distribution of the wave function as seen from the wave functions in Figs. 12 and 13 and therefore also influences the diamagnetic shifts in Faraday configuration. The largest effective vertical extension is expected for the symmetric molecule structure just discussed, leading to the largest diamagnetic shift. For a molecule composed of dot structures with different ground state energies, the extension will be reduced, leading to a smaller diamagnetic shift. For the wide barrier structures which do not show a simple doublet splitting, but exhibit complicated fine structure patterns consisting of up to eight emission lines, it is rather difficult to determine a diamagnetic shift. It has been estimated by averaging the energies of all spectral features observed at a certain B.[45] The resulting changes originating from the variations of the dot geometry fall into the statistics of the diamagnetic shifts, given by the bars in Fig. 40. Therefore the observed trend of the average shift lies generally outside of the bars, demonstrating clearly the influence of the barrier width variation and indicating that the effects of symmetry reductions are rather small for the molecules showing positive diamagnetic shifts.

To understand the data on a quantitative level, detailed calculations of the exciton states are required for which we need to know the precise geometry of the molecule structures as well as parameters that are related to the material composition such as masses. These parameters at present are not known to an extent sufficient to explain such sensitive effects as diamagnetic shifts quantitatively.

The qualitative picture given for the Faraday geometry diamagnetic shift results is based on specific changes of the exciton wave function spread along the molecule axis. This spread can be tested by the diamagnetic shift in the Voigt configuration given by the form Eq. (6). From this form the shift can be interpreted as a measure of how much the wave function diverges from the central barrier plane $z=0$ in the quantum dot molecules. Thus we would expect a decrease of the shift in going from wide to narrow barriers. Still the shift has to remain much larger for the narrow barrier molecules than for the isolated dots. The corresponding data up to $B=8$ T for different barrier samples are shown in the inset of Fig. 25. For the 7- and 8-nm-wide barrier samples the shifts are comparable and are almost 0.25 meV, while for the 4 nm barrier sample the shift is reduced to ~0.18 meV, indeed confirming the reduction of the wave function extension with barrier width. On the other hand the shift is still significantly more than twice the shift in the single dots, also for the narrow barrier sample.

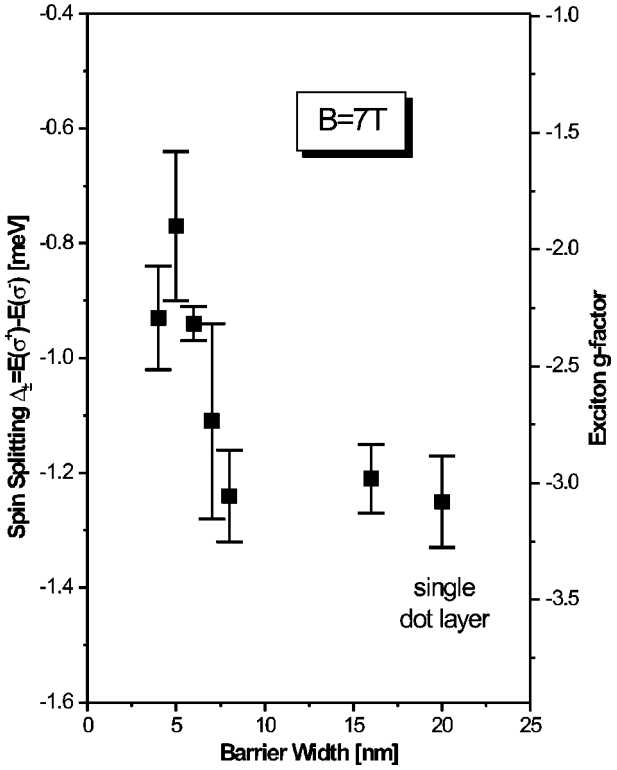

FIG. 41. Exciton spin splitting at $B=7$ T (Faraday configuration) as function of the nominal barrier width in InAs/GaAs quantum dot molecules. The right axis gives the corresponding exciton g factors. Each symbol is obtained by averaging the data of about ten different molecule structures. The bars give the variations of the splittings for the different structures with a given barrier width.

E. Exciton spin splittings

Figure 41 shows the barrier width dependence of the exciton spin splitting $\Delta_{\pm}=E(\sigma^{+})-E(\sigma^{-})$ at $B=7$ T as compared to the splitting in the quantum dot reference sample. The right-hand scale gives the exciton g factor g_X derived from these splittings by $g_X=\Delta_{\pm}/(\mu_B B)$, where μ_B is the Bohr magneton. Again we point out that data are shown only for samples that exhibit a doublet splitting in magnetic field in conjunction with a linear dependence of the splitting on B. Thus we restrict attention to the low-field regime $\leqslant 8$ T, where nonlinearities of the spin splitting are not important.

The bars denote the variation of the splitting for a given barrier width. For the single dot sample, we find a spin splitting of ~−1.2 meV, similar to the value for the 16 nm sample. Within the statistical variations this value is identical to the splittings for the 7 and 8 nm samples. For the narrow barrier samples we find a considerable increase of the split-

ting: For a 5 nm barrier the average value at 7 T is −0.8 meV only, while for the 4 nm barrier we find that the splitting decreases to slightly more than −1 meV.

The exciton g factor is obtained by averaging the electron and hole g factors over the quantum dots and the barriers with the weights given by the respective parts of the wave functions in each heterostructure component. The nonmonotonic dependence of the spin splitting on barrier width prevents its simple explanation, which also is hampered by the restricted knowledge of molecule parameters. Qualitatively the behavior can be understood in the following way, where we resort in part to the considerations for the diamagnetic shift.

For $In_xGa_{1-x}As/GaAs$ quantum wells with an In content ~10% a systematic increase of the exciton g factor has been found with increasing well width w. This width dependence arises from band mixing effects which are proportional to $1/w^2$. On the other hand, the subband splitting also increases as $1/w^2$, but the band mixing effects turn out to be dominant, so that as a net effect the g factor follows a dependence proportional to $1/w^2$.[46] For very narrow wells the g factor is negative, passes through zero for a width of about 8 nm, and becomes positive for wide barriers.

Increasing well width corresponds to some extent to a reduction of the barrier width in the quantum dot molecules: for wide barriers the amplitude of the exciton wave function in the barrier is close to zero. Obviously the compositions of the two quantum dots are similar, so that the g-factor contributions from the two dots will be roughly identical and will add up to about that in a single dot. The vertical coherence volume of the wave function in effect becomes larger for smaller barrier widths, for which there is a significant penetration of the wave function into the barrier. The barrier, which in effect is InGaAs as well due to intermixing, will therefore also contribute to the g factor. Treating the penetration in lowest approximation as an increase of the exciton wave-function in a homogeneous material, we would expect a reduction of the g factor for wider barriers as seen for the quantum wells, offering an explanation for the observed experimental trend in the molecules.

For clarity, we want to point out that even though this dependence of the spin splitting on barrier width is a further indication for coherent coupling of the quantum dots, it does not represent a conclusive proof in itself. With increasing barrier width a systematic variation of one of the parameters that determine conduction and valence band structure such as strain might occur, which could contribute also to the described variation of the exciton g factor. Only from the entirety of observations on the InAs/GaAs quantum dot molecules can we safely conclude that there is an electronic coupling of the dot structures, or in other words, among the spectroscopic results we do not find an observation that would contradict electronic coupling.

VI. SUMMARY AND OUTLOOK

The aim of this paper was to develop a detailed picture of the exciton fine structure in coupled quantum dots by single molecule spectroscopy. From anticrossings observed in the magnetic field dispersion of the exciton fine structure for wide barrier molecules, a quantum mechanically coherent coupling of the dots has been established. The fine structure patterns depend sensitively on the details of the molecule geometry and thus vary from molecule to molecule. This conclusion has been consolidated by studies of diamagnetic shifts in these systems. The coupling can be well understood on the basis of quantum mechanical tunneling of the carriers through the molecule barrier, although we cannot exclude that also other mechanisms such as Förster resonant energy transfer or dipole-dipole interaction contribute as well.

The proof by avoided crossings does not work for the narrow barrier molecules, since the energy splitting between the exciton states is too large to induce state resonances by magnetic field. For them, however, a coupling was demonstrated recently in nonlinear optical studies of the exciton dephasing.[47] In these experiments a systematic increase of the zero-temperature homogeneous linewidth with decreasing barrier thickness was found whose details can be understood by a tunnel coupling of the dots. Systematic dependencies were obtained in these studies also for other quantities characterizing the exciton dephasing, such as the zero-phonon line weight or activation energies. Tunneling was indicated also by measurements of the exciton lifetime, in which a considerable reduction of the lifetime was observed due to the increase of its coherence volume in the molecules and the resulting superradiance.[48]

The picture of the exciton fine structure developed here might give a very diverse impression of the coupling of the dots forming the molecule structures. However, we have been addressing the smallest possible energy scale of fine structure effects, which occur in the meV range (neglecting potentially even smaller effects such as the hyperfine interaction of carriers with lattice nuclei). When studying effects on larger energy scales the picture does not appear to be so multifaceted, as seen from the energy splitting between "bonding" and "antibonding" exciton states. Still also this splitting varies considerably since it depends exponentially on structural details of the barrier such as width and height.

Here we want to stress again that for quantum mechanical coupling the two quantum dot structures in the molecule do not have to be identical on an atomistic level, which of course will never be the case. Instead, as criterion for significant coupling one might loosely formulate that the kinetic energy reduction due to penetration of the carrier wave functions through the barrier is bigger than the difference in energy that arises from dissimilarity of the quantum dots.

Still many questions need to be addressed for the molecule structures: in the linear regime, only photoluminescence spectroscopy has been performed up to now, from which the exciton spectrum cannot be derived. For this purpose, photoluminescence excitation experiments need to be performed.[49] Independent of the specific technique applied, interband optics always addresses the combined properties of electron and hole. Since in the molecules electron and hole levels might be subject to considerable differences in their tunnel coupling, there is huge demand to address electrons and holes separately, which requires far infrared spectroscopy.

On the theory side, also quite some effort needs to be undertaken to obtain a better understanding of the confined

electron and hole states in the molecule structures. Here we used an effective mass model, which might be too simple for calculating the exciton states on a quantitative level, in particular the absolute emission energies. But on the other hand, it allows us to obtain systematic insight into the physics of the interplay of tunnel coupling and Coulomb interaction. Further, it allowed us to do modeling of fine structure effects. For calculating the molecular levels, other techniques employing $\mathbf{k}\cdot\mathbf{p}$, tight binding, or pseudopotential methods are clearly superior, but at the moment might not allow us to address such small effects as the exciton fine structure (see Refs. 15–18 for an overview). However, these techniques also need reliable input from a structural analysis of the molecules as they do not include a microscopic modeling of the epitaxial growth of the structures.

The results reported here also affect strongly considerations of the semiconductor-based generation of polarization-entangled photon pairs.[50] For their creation also the decay of two-exciton complexes in tunnel-coupled quantum dots has been suggested.[51] The presented data show that such a goal will not be easily achieved, since symmetry reductions of the molecule structure will lead to a fine structure splitting, which makes the two photons that are emitted in the biexciton decay cascade distinguishable, thus leading to a breakdown of entanglement. Such deviation from cylindrical symmetry also prevented up to now the observation of a polarization entanglement in the biexciton photon cascade of single quantum dots.[52]

Even if the symmetry were perfect, it seems doubtful that a polarization entanglement could be obtained from the biexciton decay. In contrast to the generation of entangled photons through parametric down-conversion[53] of an intense laser beam in an optically nonlinear crystal, where the two photons are generated simultaneously, here the generation is truly sequential. First one electron-hole pair of the biexciton complex decays, then the next one, both on time scales of about a nanosecond, which is the typical radiative decay time of excitons in self-assembled quantum dots.[54] Since exciton dephasing in these systems is ultimately limited by the radiative decay,[55] decoherence between the first and second electron-hole pair recombinations might occur. This potentially destroys the quantum mechanical coherence of the photon pair, even though classical correlations between the photon polarizations might be preserved, as typical spin flip times are much longer than the radiative decay time in zero-dimensional semiconductor systems such as quantum dots[56,57] and molecules. Here implementation of the dot structures into a resonator with the correponding shortening of the radiative lifetime might offer the chance to create a polarization entanglement, before coherence-breaking mechanisms set in.

The answer to these questions is also of crucial importance for the relation of coupled dot structures to the field of quantum information processing that has been developed in Ref. 14. Assuming a situation of perfect tunneling for electron and hole in a symmetric quantum dot molecule, it has been shown that the excitons represent strongly entangled isospin states, since in the wave function forms of Eqs. (1) all electron-hole configurations (which are a complete basis set) contribute significantly. Every symmetry reduction will lead to a reduction of entanglement, demonstrated recently for molecules with an ideal InAs/GaAs material composition.[18] As was shown in Sec. IV, the most general representation of the entangled excitons as nonfactorable electron hole states is given by

$$|\Psi_i\rangle = \sum_{j=1}^{4} c_{ij}|G_j\rangle, \tag{10}$$

where the G_j are the independent particle electron-hole arrangements in the localized basis. The coefficients $c_{ij}(\Sigma|c_{ij}|^2=1)$ depend on the detailed molecule geometry. If, for example, the hole is localized in one of the dots (dot 0) and only the electron tunnels through the barrier, two states are formed,

$$|S_1'\rangle = c_{11}|0,0\rangle + c_{12}|1,0\rangle,$$

$$|S_2'\rangle = c_{21}|0,0\rangle - c_{22}|1,0\rangle. \tag{11}$$

Clearly these states can be factorized, and the entanglement completely breaks down. In case of such an asymmetry, it might be compensated for, however, by applying an electric field along the molecule axis, by which the carrier distribution might be controlled on a detailed level.

Further, our results show that despite the high quality of the present molecules the obtained control of fabrication might not be sufficient yet to construct quantum functional devices by controlled coupling of self-assembled semiconductor quantum dots. For technological applications in which truly quantum mechanical effects are exploited, one would like to have virtually identical quantum dots to form molecules with complex geometries.

ACKNOWLEDGMENTS

This work was supported by the Deutsche Forschungsgemeinschaft within the research program "Quantum Optics in Semiconductor Nanostructures." It was also supported by the QuIST program of DARPA, by the NRC-Helmholtz Joint Research program, by the "Canadian European Research Initiative on Nanostructures," CERION, of the EC, by the ONR Nanoscale Electronics program, and by the BMBF nanoquit program.

*Electronic address: gerhard.ortner@physik.uni-dortmund.de
†On leave from the Institute of Physics, St. Petersburg State University, 198504, Russia.
‡On leave from the Institute of Solid State Physics, Russian Academy of Sciences, Chernogolovka, 432132, Russia.
§Present address: Cyrium Technologies, Ottawa, ON, Canada.

[1] See, for example, G. Bastard, *Wave Mechanics Applied to Semiconductor Heterostructures* (Halstead, New York, 1988); M. Jaros, *Physics and Applications of Semiconductor Microstructures* (Clarendon Press, Oxford, 1989); C. Weisbuch and B. Vinter, *Quantum Semiconductor Structures* (Academic Press, New York, 1991); M. Kelly, *Low-Dimensional Semiconductors* (Clarendon Press, Oxford, 1995).

[2] D. Bouwmeester, A. Ekert, and A. Zeilinger, *The Physics of Quantum Information* (Springer, Berlin, 2000).

[3] A. Barenco, D. Deutsch, A. Ekert, and R. Jozsa, Phys. Rev. Lett. **74**, 4083 (1995); A. Imamoglu, D. D. Awschalom, G. Burkard, D. P. DiVincenzo, D. Loss, M. Sherwin, and A. Small, *ibid.* **83**, 4204 (1999).

[4] G. Schedelbeck, W. Wegscheider, M. Bichler, and G. Abstreiter, Science **278**, 1792 (1997).

[5] T. Fujisawa, T. H. Oosterkamp, W. G. van der Wiel, B. W. Broer, R. Aguado, S. Tarucha, and L. P. Kouwenhoven, Science **282**, 932 (1998).

[6] R. H. Blick, D. Pfannkuche, R. J. Haug, K. von Klitzing, and K. Eberl, Phys. Rev. Lett. **80**, 4032 (1998); R. H. Blick, D. W. van der Weide, R. J. Haug, and K. Eberl, *ibid.* **81**, 689 (1998); A. W. Holleitner, R. H. Blick, A. K. Hüttel, K. Eberl, and J. P. Kotthaus, Science **297**, 70 (2002).

[7] See, for example, L. Jacak, P. Hawrylak, and A. Wojs, *Quantum Dots* (Springer, Berlin, 1997); D. Bimberg, N. N. Ledentsov, and M. Grundmann, *Quantum Dot Heterostructures* (John Wiley & Sons, London, 1998).

[8] Q. Xie, A. Madhukar, P. Chen, and N. P. Kobayashi, Phys. Rev. Lett. **75**, 2542 (1995); G. S. Solomon, J. A. Trezza, A. F. Marshall, and J. S. Harris, *ibid.* **76**, 952 (1996).

[9] P. Boucaud, K. S. Gill, J. B. Williams, M. S. Sherwin, W. V. Schoenfeld, and P. M. Petroff, Appl. Phys. Lett. **77**, 510 (2000).

[10] G. Sek, K. Ryczko, J. Misiewicz, M. Bayer, F. Klopf, J. P. Reithmaier, and A. Forchel, Solid State Commun. **117**, 401 (2001).

[11] I. Shtrichman, C. Metzner, B. D. Gerardot, W. V. Schoenfeld, and P. M. Petroff, Phys. Rev. B **65**, 081303 (R) (2002).

[12] S. Fafard, M. Spanner, J. P. McCaffrey, and Z. R. Wasilewski, Appl. Phys. Lett. **76**, 2268 (2000).

[13] Overviews of single dot spectroscopy are given, for example, in A. Zrenner, J. Chem. Phys. **112**, 7790 (2000); D. Gammon and D. G. Steel, Phys. Today **55** (10), 36 (2002).

[14] M. Bayer, P. Hawrylak, K. Hinzer, S. Fafard, M. Korkusinski, Z. R. Wasilewski, O. Stern, and A. Forchel, Science **291**, 451 (2001).

[15] G. W. Bryant, Phys. Rev. B **48**, 8024 (1993).

[16] L. R. C. Fonseca, J. L. Jimenez, and J. P. Leburton, Phys. Rev. B **58**, 9955 (1998).

[17] W. Sheng and J.-P. Leburton, Appl. Phys. Lett. **78**, 1258 (2001); Phys. Rev. B **64**, 153302 (2002); Phys. Rev. Lett. **88**, 167401 (2002); Phys. Rev. B **67**, 125308 (2003).

[18] G. Bester, J. Shumway, and A. Zunger Phys. Rev. Lett. **93**, 047401 (2004); and (private communication).

[19] G. Ortner, M. Bayer, A. Larionov, V. B. Timofeev, A. Forchel, Y. B. Lyanda-Geller, T. L. Reinecke, P. Hawrylak, S. Fafard, and Z. Wasilewski, Phys. Rev. Lett. **90**, 086404 (2003).

[20] L. Goldstein, F. Glas, J. Y. Marzin, M. N. Charasse, and G. LeRoux, Appl. Phys. Lett. **47**, 1099 (1985).

[21] S. Fafard, Z. R. Wasilewski, C. N. Allen, D. Picard, M. Spanner, J. P. McCaffrey, and P. G. Piva, Phys. Rev. B **59**, 15 368 (1999).

[22] I. Kegel, T. H. Metzger, A. Lorke, J. Peisl, J. Stangl, G. Bauer, J. M. Garcia, and P. M. Petroff, Phys. Rev. Lett. **85**, 1694 (2000); D. M. Bruls, J. W. A. M. Vugs, P. M. Koenraad, H. W. M. Salemink, J. H. Wolter, M. Hopkinson, M. S. Skolnick, Fei Long, and S. P. A. Gill, Appl. Phys. Lett. **81**, 1708 (2002); D. M. Bruls, P. M. Koenraad, H. W. M. Salemink, J. H. Wolter, M. Hopkinson, and M. S. Skolnick, *ibid.* **82**, 3758 (2003).

[23] J. P. McCaffrey, M. D. Robertson, S. Fafard, Z. R. Wasilewski, E. M. Griswold, and L. D. Madsen, J. Appl. Phys. **88**, 2272 (2000).

[24] A. Kuther, M. Bayer, A. Forchel, A. Gorbunov, V. B. Timofeev, F. Schäfer, and J. P. Reithmaier, Phys. Rev. B **58**, R7508 (1998).

[25] Since the relaxation from the *p*-shell into the *s*-shell molecule states is fast, one observes for the *p* shell the typical state filling effects as for the quantum dot reference. For the 5 nm barrier sample in Fig. 2, for example, first the "bonding" *p*-shell state becomes occupied with increasing excitation, and only after its filling also the "antibonding" *p*-shell state becomes populated.

[26] The precise linewidth is hard to determine since often a few fine structure lines with small energy splittings in between contribute to the emission, as in case of the ground state emission (see discussion in text). Within this multiplet, no spectral filtering through polarization selection is possible, since the involved states in most cases are not pure angular momentum states.

[27] The temperature increase leads to a low-energy shift of the quantum dot molecule emission due to the related band gap reduction.

[28] We note that in Ref. 14 we had erroneously interpreted the increase of intensity from the higher-lying molecule exciton state upon increasing temperature as caused by thermal excitation. This was based on the absence of significant emission from multiexciton complexes while increasing simultaneously the excitation power. The origin of the emission intensity dependencies on temperature and excitation is not yet fully understood. A simple estimate shows that the change of occupation probabilities by a temperature increase from 10 to 50 K is not sufficient to explain the changes of the ratio of emission intensity from "bonding" and "antibonding" states in the spectra.

[29] We note that for a given barrier width there is also a weak correlation between the absolute energies of "bonding" and "antibonding" states and the energy splitting between them: the higher the center of gravity of the line energies is, the larger is the tunnel splitting. This correlation can be easily understood, since the tunnel matrix element increases (leading to a larger tunnel splitting) for smaller energy separation from the top of the barrier, i.e., the barrier height (assuming a constant tunnel barrier height for simplicity).

[30] Y. B. Lyanda-Geller, T. L. Reinecke, and M. Bayer, Phys. Rev. B **69**, 161308(R) (2004).

[31] M. Bayer, G. Ortner, O. Stern, A. Kuther, A. A. Gorbunov, A. Forchel, P. Hawrylak, S. Fafard, K. Hinzer, T. L. Reinecke, S. N. Walck, J. P. Reithmaier, F. Klopf, and F. Schäfer, Phys. Rev. B **65**, 195315 (2002); M. Bayer, A. Kuther, A. Forchel, A. Gorbunov, V. B. Timofeev, F. Schäfer, J. P. Reithmaier, T. L. Reinecke, and S. N. Walck, Phys. Rev. Lett. **82**, 1748 (1999).

[32] G. Bester, S. Nair, and A. Zunger, Phys. Rev. B **67**, 161306

(2003).

[33] Note that the real molecule structure most likely will not have such inversion symmetry due to the complicated strain distribution around the dot structures (see also text).

[34] A lateral displacement would also have pronounced effects on the interaction of molecule states that arise from quantum dot states with different angular momenta. For structures without displacement angular momentum remains a good quantum number. As a consequence *s*- and *p*-shell molecule states would cross each other when coming into resonance. This could be achieved, for example, for the "antibonding" *s*-shell and the "bonding" *p*-shell exciton state when varying the width of the separating barrier. Introducing a lateral displacement breaks the rotational symmetry leading to a mixing of states with different angular momenta, so that these two states would avoid each other when brought into resonance

[35] See, for example, X. Marie, T. Amand, J. Barrau, P. Renucci, P. Lejeune, and V. K. Kalevich, Phys. Rev. B **61**, 11 065 (2000), and references therein.

[36] We note that there has been a report on a negative diamagnetic shift of the ground state exciton emission for self-assembled quantum dots. The results have been obtained by photoluminescence spectroscopy up to $B=60$ T on a dot array with a rather large inhomogeneous broadening (Ref. 37). This finding was attributed to an increase of the exciton binding energy by B which is larger than the increase of geometric confinement by the magnetic field acting. In the analysis of such data one has to be careful how the field application affects carrier capture into the dot structures. To the best of our knowledge, in measurements on self-assembled single dots with clearly superior resolution only positive diamagnetic shifts have been observed so far. Negative diamagnetic shifts seem possible only for quantum dots in the weak confinement regime, where Coulomb dominates over the geometric confinement.

[37] R. K. Hayden, K. Uchida, N. Miura, A. Polimeni, S. T. Stoddart, M. Henini, L. Eaves, and P. C. Main, Physica B **246-247**, 93 (1998).

[38] See, for example, G. Kioseoglou, H. D. Cheong, H. A. Nickel, A. Petrou, B. D. McCombe, and W. Schaff, Phys. Rev. B **61**, 4780 (2000); S. Glasberg, G. Finkelstein, H. Shtrikman, and I. Bar-Joseph, *ibid.* **59**, R10 425 (1999), and references in these publications.

[39] See, for example, S. N. Walck and T. L. Reinecke, Phys. Rev. B **57**, 9088 (1998).

[40] We note that only fields up to about 15 T have been used in these studies.

[41] See, for example, N. J. Traynor, R. J. Warburton, M. J. Snelling, and R. T. Harley, Phys. Rev. B **55**, 15 701 (1997).

[42] A. Babinski, G. Ortner, S. Raymond, M. Potemski, M. Bayer, P. Hawrylak, A. Forchel, Z. Wasilewski, and S. Fafard (unpublished).

[43] For completeness we note that up to now we have performed only a few studies of the fine structure of the "antibonding" exciton state in the narrow barrier molecules. In all of them, also the high-energy line showed a doublet splitting, as we would expect, since as in the case of $|S_1\rangle$ and $|S_2\rangle$, the energy separation between $|S_3\rangle$ and $|S_4\rangle$ has become so large that a magnetic field with strengths comparable to the ones available here cannot bring these levels in resonance.

[44] S. N. Walck and T. L. Reinecke, Phys. Rev. B **57**, 9088 (1998), and references therein; M. Bayer, S. N. Walck, T. L. Reinecke, and A. Forchel, *ibid.* **57**, 6584 (1998).

[45] Alternately, rough estimates for the diamagnetic shift can be obtained by identifying pairs of lines which converge for zero magnetic field after fitting crossing lines to the data at the anticrossing points in the magnetic field dispersions. When doing so, for example, for QDM3 and QDM4 in Fig. 18, one also obtains diamagnetic shift values which fall into the statistics of the data for the respective barrier widths.

[46] R. Kotlyar, T. L. Reinecke, M. Bayer, and A. Forchel, Phys. Rev. B **63**, 085310 (2001), and references therein.

[47] P. Borri, W. Langbein, U. Woggon, M. Schwab, M. Bayer, S. Fafard, Z. Wasilewski, and P. Hawrylak, Phys. Rev. Lett. **91**, 267401 (2003).

[48] C. Bardot, M. Schwab, M. Bayer, S. Fafard, Z. Wasilewski, and P. Hawrylak (unpublished).

[49] In the present samples photoluminescence excitation studies were hampered because of the structure growth on *n*-doped substrates. From this doping a significant background arises in the energy range of the excited molecule states, from which the molecule signal cannot be separated reliably.

[50] O. Benson, C. Santori, M. Pelton, and Y. Yamamoto, Phys. Rev. Lett. **84**, 2513 (2000).

[51] O. Gywat, G. Burkard, and D. Loss, Phys. Rev. B **65**, 205329 (2002).

[52] C. Santori, D. Fattal, M. Pelton, G. S. Solomon, and Y. Yamamoto, Phys. Rev. B **66**, 045308 (2002); E. Moreau, I. Robert, L. Manin, V. Thierry-Mieg, J. M. Gérard, and I. Abram, Phys. Rev. Lett. **87**, 183601 (2001); R. M. Thompson, R. M. Stevenson, A. J. Shields, I. Farrer, C. J. Lobo, D. A. Ritchie, M. L. Leadbeater, and M. Pepper, Phys. Rev. B **64**, 201302 (2001).

[53] See, for example, G. Weihs, T. Jennewein, C. Simon, H. Weinfurter, and A. Zeilinger, Phys. Rev. Lett. **81**, 5039 (1998), and references therein. An overview of the potential application of entangled photons, for example in metrology, is given in A. Sergienko, *Quantum Metrology with Entangled Photons*, in *Proceedings of the International School of Physics "Enrico Fermi", Course CXLVI*, edited by T. J. Quinn, S. Leschiutta, and P. Tavella (IOS Press, Amsterdam, 2001).

[54] M. Paillard, X. Marie, E. Vanelle, T. Amand, V. K. Kalevich, V. M. Ustinov, and N. N. Ledentsov, Appl. Phys. Lett. **76**, 76 (2000).

[55] W. Langbein, P. Borri, U. Woggon, V. Stavarache, D. Reuter, and A. Wieck, Phys. Rev. B **70**, 033301 (2004).

[56] M. Paillard, X. Marie, P. Renucci, T. Amand, A. Jbeli, and J. M. Gerard, Phys. Rev. Lett. **86**, 1634 (2001).

[57] L. M. Woods, T. L. Reinecke, and Y. Lyanda-Geller, Phys. Rev. B **66**, 161318 (R) (2002).